cell-surface heparan sulfate proteoglycans (HSPGs) that would modulate the cholesterol-effluxing ability of apoE.[21–23]

Methods

Materials

RAW264.7 cells and HeLa cells were purchased from American Type Culture Collection (Manassas, Va) and the Health Science Research Resources Bank (Osaka, Japan), respectively. Adenoviral vectors AdE2, AdE3, and AdE4,[14] encoding apoE2, E3, and E4 isoform cDNA, respectively, were used to express human apoE isoforms. AdLacZ[14] was used as a control adenovirus. Acetylated LDL was prepared from normal human LDL by following a method previously described.[24]

Determination of Multiplicity of Infection for Efficient Gene Delivery

RAW264.7 cells were infected with either 0, 80, or 240 multiplicity of infection (MOI) of AdLacZ, and HeLa cells were infected with either 0, 1, or 100 MOI of AdLacZ. Forty-eight hours after infection, cells were fixed with 0.5% glutaraldehyde and incubated overnight at 37°C with a solution containing 5 mmol/L $K_3Fe(CN)_6$, 5 mmol/L $K_4Fe(CN)_6$, 1 mmol/L $MgCl_2$, and 1 mg/mL 5-bromo-4-chloro-3-indolyl β-D-galactopyranoside (X-gal).

Expression of ApoE Isoforms in RAW264.7 Cells by Adenoviral Vectors

RAW264.7 cells were cultured with or without 1 mmol/L β-DX; infected with 240 MOI of AdE2, AdE3, AdE4, or AdLacZ; and cholesterol-loaded with 100 μg/mL protein of acetylated LDL. Twenty-four hours later, cells were washed 3 times with PBS and cultured further for 48 hours in Dulbecco's modified Eagle's medium (DMEM) supplemented with 0.3% bovine serum albumin (BSA), and 0.3 mmol/L 8-Br-cAMP, with or without 1 mmol/L β-DX. For Western blot analysis, cells lysed in sample buffer and cell medium were stocked at −80°C. For Northern blotting, 25 μg of cellular total RNA purified by the acid guanidinium-phenol-chloroform method was electrophoresed and blotted to nylon membranes, which were then hybridized with digoxigenin-labeled apoE3 cDNA probe followed by incubation with alkaline phosphatase–conjugated anti-digoxigenin antibody. The signals were detected with a chemiluminescence method, and the intensities of bands were quantified by using NIH Image software. After stripping the apoE probes, the membranes were reprobed with mouse glyceraldehyde-3-phosphate dehydrogenase (GAPDH) cDNA.

Studies With Endogenous ApoE Expression

RAW264.7 cells, cultured with or without 1 mmol/L β-DX for 48 hours, were either infected with 240 MOI of each adenoviral vector or left uninfected with an adenoviral vector and cholesterol-loaded with 100 μg/mL protein of acetylated LDL. For cholesterol-unloaded control cells, RAW264.7 cells were neither cholesterol-loaded nor infected with adenovirus. After another 24 hours, the cells were washed 3 times with PBS and cultured for an additional 36 hours in DMEM supplemented with 0.3% BSA and 0.3 mmol/L 8-Br-cAMP, with or without 1 mmol/L β-DX, after which lipid extraction from cells was performed as described below. To evaluate the effect of 8-Br-cAMP on cholesterol efflux, some plates were cultured without 8-Br-cAMP and β-DX.

Studies With Exogenous ApoE

HeLa cells were either uninfected or infected with 100 MOI of each adenoviral vector. Twenty-four hours later, cells were washed 3 times with PBS and cultured for another 48 hours in DMEM supplemented with 0.3% BSA. The medium was then harvested, quickly centrifuged, and diluted with DMEM to make the final apoE concentration 50 μg/mL. The medium harvested from cells treated with AdLacZ or no adenovirus was diluted at the average ratio of those of apoE isoforms. The medium was stocked at 4°C for up to 3 days until use in the experiments described below. Aliquots of the medium were subjected to fast protein liquid chromatography (FPLC) on a Superose 6 column (Pharmacia LKB Biotechnology), and 2 adjacent fractions were pooled together and subjected to Western blot analysis.

RAW264.7 cells were cultured with or without 1 mmol/L β-DX, and 48 hours later, 100 μg/mL acetylated LDL was added. After another 24 hours, the cells were washed 3 times with PBS and cultured in the medium obtained from HeLa cells in the presence of 0.3 mmol/L 8-Br-cAMP and 0.3% BSA, with or without 1 mmol/L β-DX. Some plates were cultured in the absence of 8-Br-cAMP and β-DX to assess the role of 8-Br-cAMP in cholesterol efflux. Thereafter, for the measurement of cellular lipid contents, cells were cultured for 36 hours. For the detection of cell surface–bound apoE, the cells were then cultured for 24 hours, washed 3 times with PBS, and incubated for another 4 hours with 0.5 mL DMEM with or without the addition of 2 U/mL heparinase I. The medium was quickly centrifuged, and the supernatant was preserved for Western blot analysis. The cells were harvested, and the cellular protein concentration was measured by the Lowry method.

Extraction and Quantification of Lipid From Cells

Cells were collected into tubes and washed 3 times with PBS. After a hexane/isopropanol mixture (3:2, vol/vol) was added, the tubes were vortexed and placed at room temperature for 30 minutes. After centrifugation, the supernatant was transferred to glass tubes and dried under nitrogen gas, followed by the measurement of cholesterol content; the pellet was used for measurement of cellular protein content. Total cholesterol (TC) and free cholesterol (FC) were measured by enzymatic methods, and protein concentration was measured by the Lowry method. After the adjustment of cellular TC and FC contents for cellular protein, the cellular esterified cholesterol (EC) content was calculated by subtracting the FC content value from the TC content value.

Western Blotting of ApoE

The medium collected from RAW264.7 cells, adjusted for the protein concentration of the cells, or aliquots of FPLC fractions were subjected to SDS-polyacrylamide gel electrophoresis. Proteins were blotted to nitrocellulose membranes and reacted with goat anti-human apoE polyclonal antibody, followed by incubation with peroxidase-labeled rabbit anti-goat IgG antibody. The protein bands were visualized with 4-chloro-1-naphthol as the substrate.

Results

Determination of MOI for Efficient Gene Delivery

The efficiency of gene delivery with adenoviral vectors was determined by X-gal staining of cells infected with AdLacZ (Figure 1). In RAW264.7 cells, a few faintly stained cells were observed even at an MOI of 0, owing to the endogenous activity of galactosidase. As MOI increased, the proportion of stained cells increased and the intensity of the staining became stronger. At an MOI of 240, maximal gene expression (≈70%) was observed. In HeLa cells, 100% of staining was observed at an MOI of 100. In consequence, for the subsequent experiments, an MOI of 240 and 100 was used for RAW264.7 cells and HeLa cells, respectively.

Expression of ApoE Isoforms in RAW264.7 Cells With Adenoviral Vectors

To examine whether infection at the same MOI of adenovirus resulted in the same level of expression, total RNA purified from RAW264.7 cells infected with either AdE2, E3, or E4 was subjected to Northern blot analysis (Figure 2A). The relative ratios of apoE mRNA to GAPDH mRNA were 1.12, 1.00, and 1.02 for apoE2, apoE3, and apoE4, respectively.

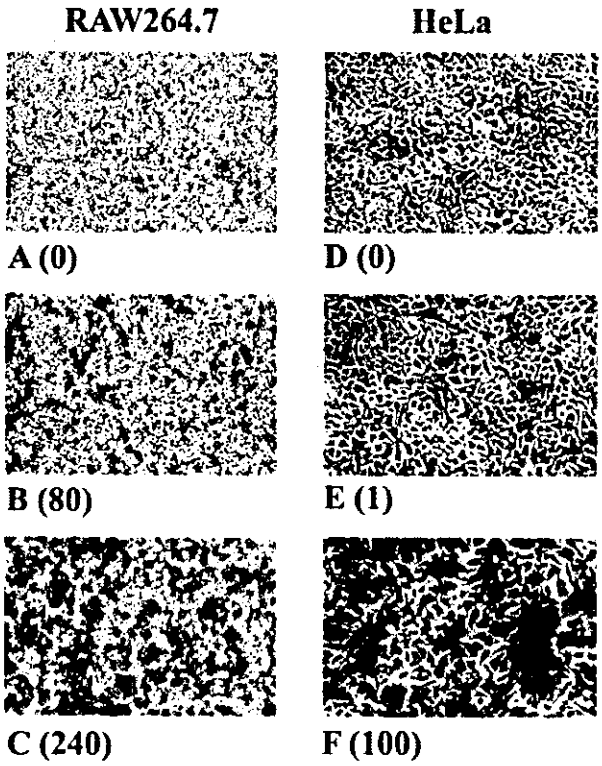

Figure 1. X-gal staining of RAW264.7 and HeLa cells. RAW264.7 cells and HeLa cells were infected with AdLacZ at different MOIs and subjected to X-gal staining. A, B, and C: RAW264.7 cells; D, E, and F: HeLa cells. The values of MOI are indicated in parentheses.

Western blot analysis of the medium revealed no difference in the protein levels among the apoE isoforms in the presence of β-DX (Figure 2B). However, without the addition of β-DX, little difference was observed in protein levels among the isoforms (Figure 2C); the relative apoE protein

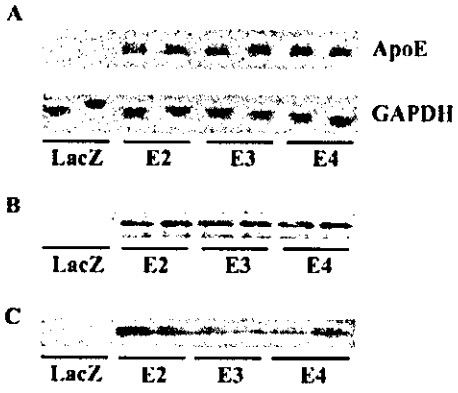

Figure 2. A: Northern blot analysis of RAW264.7 cells infected with apoE adenoviruses. Twenty-five micrograms of total cellular RNA separated on a gel and blotted to a nylon membrane was probed with human apoE cDNA or mouse GAPDH cDNA. B, C: Western blot analysis of apoE protein from the medium harvested from RAW264.7 cells infected with apoE adenoviruses with (B) or without (C) β-DX. LacZ, E2, E3, E4 indicate samples from cells infected with AdLacZ, AdE2, AdE3, and AdE4, respectively.

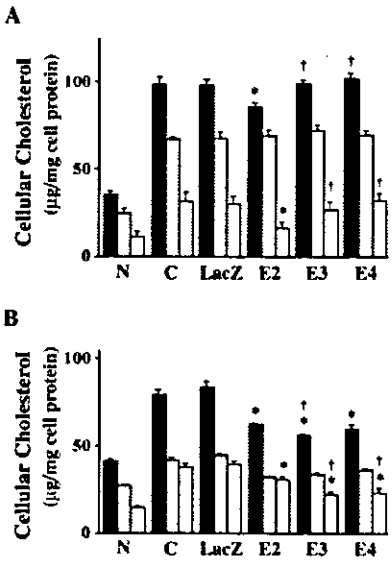

Figure 3. Cholesterol efflux by endogenous apoE. RAW264.7 cells were infected with adenoviral vectors and loaded with cholesterol, after which lipid extraction was performed. A and B represent the results without and with treatment of the cells by β-DX, respectively. N indicates cells untreated with acetylated LDL and adenovirus. C, Cholesterol-loaded cells untreated with adenovirus. LacZ, E2, E3, E4 indicate cholesterol-loaded cells treated with AdLacZ, AdE2, AdE3, and AdE4, respectively. Closed bars represent TC/cell protein, stippled bars represent FC/cell protein, and open bars represent EC/cell protein. Data are mean±SEM (n=6). *$P<0.05$ compared with both C and LacZ; †$P<0.05$ compared with E2.

levels in the medium of apoE2 and apoE4 versus apoE3 were 1.93 and 1.31, respectively.

Effect of Endogenous ApoE Expression on Cellular Cholesterol

The cholesterol loading of RAW264.7 cells resulted in a 2- to 3-fold increase in cellular TC, FC, and EC contents (Figure 3). In the absence of β-DX, a significant reduction in the cellular TC and EC content was attained in cells expressing apoE2 (12.4% and 44.9% reduction for TC and EC, respectively, compared with LacZ) (Figure 3A). ApoE3 reduced cellular cholesterol content to a lesser degree than did apoE2, which was not significantly different from control. ApoE4 did not result in the reduction of cellular cholesterol. In the absence of 8-Br-cAMP, no change in cellular cholesterol was observed in cells expressing any apoE isoform (please see Figure IA at http:atvb.ahajournals.org). Interestingly, in the presence of β-DX, all 3 apoE isoforms resulted in a significant reduction of cellular TC and EC contents (Figure 3B). Percentages for these reductions compared with LacZ control were as follows: 25.6% and 22.5% for TC and EC of apoE2, 33.2% and 43.1% for TC and EC of apoE3, and 28.7% and 40.6% for TC and EC of apoE4. In the presence of β-DX, the extent of reduction in cellular cholesterol was greatest with apoE3, followed by apoE4, and least in apoE2.

Effect of Exogenous ApoE on Cellular Cholesterol

FPLC analysis of the medium from HeLa cells infected with apoE adenovirus revealed that the apoE protein, regardless of

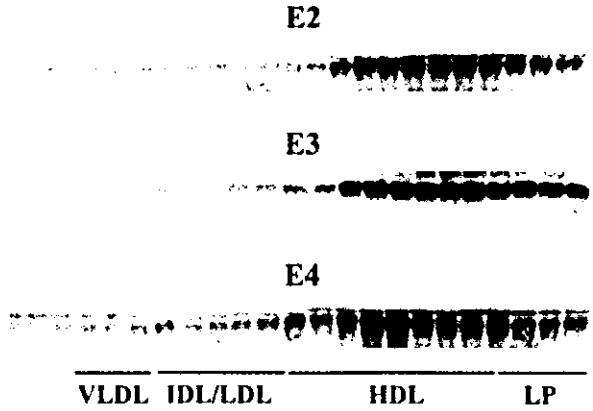

Figure 4. Distribution of apoE protein on lipoprotein particles in the medium harvested from HeLa cells infected with apoE adenovirus. E2, E3, E4 indicate samples harvested from HeLa cells infected with AdE2, AdE3, and AdE4, respectively. Lanes 4 through 6 correspond to VLDL fractions, lanes 7 through 11 to IDL/LDL fractions, lanes 12 through 19 do HDL fractions, and lanes 20 through 23 to lipid-poor fractions.

its isoform, distributed mostly on HDL and VHDL fractions and, to a lesser extent, on lipid-poor fractions (Figure 4).

In the absence of β-DX, apoE2- and E3-containing media significantly reduced cellular TC and EC contents (22.9% or 16.9% reduction for TC and 29.1% or 20.5% reduction for EC, respectively, compared with LacZ control) (Figure 5A). Medium containing apoE4 showed trends toward a reduction of TC and EC contents; however, no significant reduction was observed. When we compared the efficiency in the reduction of TC and EC among the 3 isoforms, apoE4 was less effective than apoE2 and E3, and apoE2 showed a tendency in the increased reduction for TC and EC compared with apoE3. The reduction in cellular cholesterol by apoE isoforms was not observed in the absence of 8-Br-cAMP (please see Figure IB at http://atvb.ahajournals.org).

In the presence of β-DX, all 3 exogenous apoE isoforms resulted in a significant reduction of cellular TC and EC contents (Figure 5B), which was the case with endogenous apoE isoforms. However, the differential effect among the isoforms was not found in this experiment with exogenous apoE.

Detection of Cell Surface–Bound ApoE by Using Heparinase

To elucidate whether the binding ability to cell surface HSPGs differs among apoE isoforms, RAW264.7 cells were incubated with the medium harvested from HeLa cells for 24 hours, which were then washed and incubated with 2 U/mL heparinase I. The catalyzing activity of heparinase I for HSPGs was confirmed by additional experiments with lactoferrin (data not shown). In the absence of β-DX, the amount of apoE released by heparinase I increased in the following order: E2<E3<E4 (Figure 6A and B). On the other hand, when the production of cell surface HSPGs was inhibited by β-DX, release of apoE protein from the cell surface by heparinase I was not observed (Figure 6C).

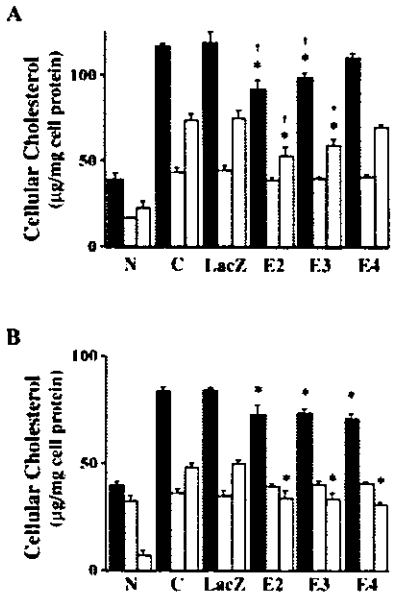

Figure 5. Cholesterol efflux by exogenous apoE. RAW264.7 cells were loaded with cholesterol by acetylated LDL and cultured in the medium containing each apoE isoform, after which lipid extraction was performed. A and B represent the results without and with treatment of the cells by β-DX, respectively. N indicates cells untreated with acetylated LDL. C, LacZ, E2, E3, E4 indicate cholesterol-loaded cells treated with the medium harvested from HeLa cells uninfected with adenovirus or infected with AdLacZ, AdE2, AdE3, and AdE4, respectively. Closed bars represent TC/cell protein, stippled bars represent FC/cell protein, and open bars represent EC/cell protein. Data are mean±SEM (n=6). *$P<0.05$ compared with both C and LacZ; †$P<0.05$ compared with E4.

Discussion

It has been difficult to induce macrophage cell lines to express any genes by the DNA transfection method. Adenoviral vectors are good tools for gene transfer into any cells that express specific integrins[25] and the coxsackievirus and adenovirus receptor.[26] Another benefit of using adenoviral vectors for gene transfer is that it is possible to make the level of expression similar among different genes by using the same promoter and infecting viruses at the same MOI. As was shown in Results, good efficiency of infection up to 70% was obtained by adenovirus-mediated gene transfer to RAW264.7 cells, and infection at the same MOI resulted in the same levels of expression among the 3 apoE isoforms. The levels of apoE protein expression analyzed with the cellular proteins were almost the same among the 3 isoforms, confirming the same levels of expression in the cells (data not shown).

Previous observations imply that HSPGs play a pivotal role in the apoE-mediated cholesterol efflux from macrophages. Lucas et al[21] clarified that HSPGs sequester apoE molecules, leading to modulation in the synthesis and secretion of apoE from the cells. Obunike et al[22] reported that the endogenously expressed apoE not only binds to cell surface HSPGs but also regulates the synthesis of HSPGs. Therefore, we explored the ability of apoE isoforms to modulate the efflux of cholesterol from macrophages with or without cell surface HSPGs.

When the production of cell surface HSPGs was inhibited, the endogenously expressed as well as exogenously derived apoE,

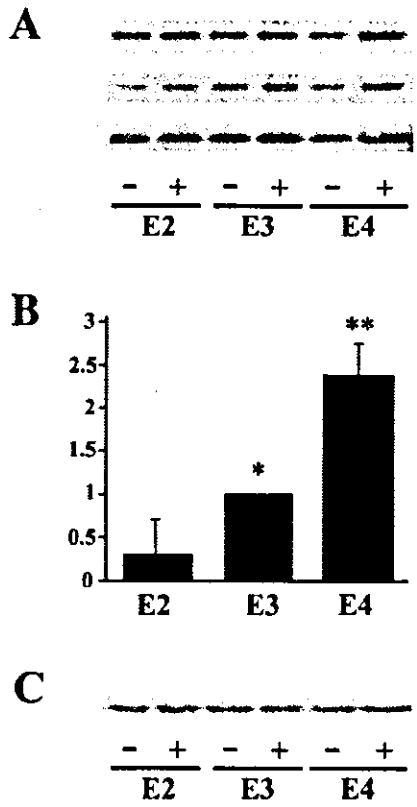

Figure 6. Release of apoE protein from the cell surface after treatment of RAW264.7 cells with heparinase I. A, Representative Western blotting analysis of the medium harvested from cells cultured without β-DX. − Indicates samples untreated with heparinase I; +, samples treated with heparinase I. B, Three independent experiments from A were subjected to densitometric analysis, and the increase in the intensity of the band from (−) to (+) was measured. The relative increment for apoE2 and E4 was calculated after setting the increment in apoE3 as 1. Data are mean±SEM. *$P<0.05$ compared with apoE2; **$P<0.01$ compared with apoE2. C, Representative Western blotting analysis of the medium harvested from cells cultured with β-DX. − Indicates samples untreated with heparinase I; +, samples treated with heparinase I.

regardless of its isoform, effectively reduced cholesterol in cholesterol-loaded RAW264.7 cells. There was no statistical difference among the exogenously derived 3 isoforms; however, a small but significant difference was observed among the 3 endogenously synthesized apoE isoforms. ApoE3 and E4 were more effective than apoE2. The probable explanation for this difference is the differential intracellular association of apoE isoforms to the ATP-binding cassette transporter, ABCA1. A recent report verified that ABCA1 plays an important role in cholesterol efflux mediated by endogenous apoE,[27] and our study clarified that ABCA1, which is induced by 8-Br-cAMP, is necessary for cholesterol efflux from RAW264.7 cells, not only by endogenous apoE but also by exogenous apoE. It is possible that endogenous apoE2 is least effective in ABCA1-mediated cholesterol efflux, leading to decreased efficiency in the efflux of cholesterol. This hypothesis needs to be tested with further experiments.

On the other hand, when the production of HSPGs was not inhibited, apoE2 reduced the cellular cholesterol content significantly, regardless of whether it was derived from outside or inside the cells. ApoE3 was less effective than apoE2 when synthesized in the cells; however, when exogenously derived, it reduced cellular cholesterol content significantly, which still showed a reduced tendency in cholesterol efflux compared with apoE2. ApoE4 had no significant effect on the cellular cholesterol content. The binding of apoE to cell surface HSPGs increased in the order E2<E3<E4. These observations, together with the findings obtained from the experiments without HSPGs, suggest that the secreted and exogenously derived apoE4 protein, as well as a portion of apoE3 protein, would be captured by the cell surface HSPGs and taken up and/or degraded by the cells. Support for this concept is the report by Lucas et al,[21] which demonstrated that the apoE sequestered in the pericellular proteoglycan matrix is susceptible to cellular degradation. Ji et al[28] reported that the binding ability of β-VLDL to HSPGs depends on the apoE isoforms in the order E4-βVLDL<E3-βVLDL=E2-βVLDL; however, the binding of purified apoE to HSPGs was not different between apoE3 and apoE4. This finding is consistent with ours, considering that the lipoproteins examined in their study are β-VLDL particles and those in ours are HDLs and lipid-poor apoEs. The size and composition of lipids of lipoprotein particles would modulate the presentation of apoE to HSPGs, thereby leading to the different binding ability to HSPGs among the different lipoprotein classes.

The LDL receptor is an another candidate that mediates the binding of apoE to the surface of macrophages[29] as well as HSPGs. The binding activity of apoE2 to the LDL receptor is <2% when compared with apoE3 and E4[12]; however, our data without HSPGs with exogenous apoE revealed that there is no difference in the efficiency of cholesterol efflux among the 3 apoE isoforms. This finding suggests that the LDL receptor is not a key player in the cholesterol efflux mediated by the cell surface-bound apoE or apoE-containing HDLs in macrophages.

The present study demonstrated that the ability of apoE to promote cholesterol efflux from macrophages is not fundamentally different among the apoE isoforms. However, in the physiological setting wherein HSPGs are produced, apoE2 is most and apoE4 least effective. Epidemiological studies have clarified that the incidence of coronary heart disease is generally lower in humans carrying at least 1 apoE2 allele than those possessing other apoE genotypes,[30] and the allele for apoE4 is an independent risk factor for coronary heart disease.[15,16] We speculate that under normolipidemic conditions, in which the insult by atherogenic lipoproteins is low, apoE2 functions most effectively for the reduction in cellular cholesterol among the 3 isoforms, thus protecting humans who possess apoE2 from atherosclerosis; on the other hand, apoE4 is least effective in the efflux and would lead to the increased atherosclerosis in humans who carry the apoE4 allele.

ApoE has been proposed to possess several biologic properties that could contribute to antiatherogenic effects.[31-34] The apoE polymorphism has been shown to affect some of these functions.[32] In addition, apoE isoforms have been proved to possess differential direct cellular functions.[35] More investigations into the differential biologic effects of the isoforms would improve our understanding of the clinical observations that identified the differential effects of apoE isoforms on atherogenesis.[36,37]

In summary, we demonstrated that the ability of apoE isoforms to promote cholesterol efflux from macrophages is fundamentally similar among the apoE isoforms, regardless of whether it is derived from outside the cell or synthesized inside the cell. Nevertheless, in the physiological setting where proteoglycans are produced by macrophages, the cell surface HSPGs would modulate the ability of apoE isoforms to promote cholesterol efflux, probably through the differential binding ability of each apoE isoform to HSPGs.

Acknowledgments

This research was supported by grant-in-aid No. 10671058 from the Ministry of Education, Science and Culture of Japan. We are greatly indebted to Daniel J. Rader for critically reading the manuscript and helpful discussions.

References

1. Glass CK, Witztum JL. Atherosclerosis: the road ahead. *Cell*. 2001;104:503–516.
2. von Eckardstein A, Nofer JR, Assmann G. High density lipoproteins and arteriosclerosis: role of cholesterol efflux and reverse cholesterol transport. *Arterioscler Thromb Vasc Biol*. 2001;21:13–27.
3. Mahley RW. Apolipoprotein E: cholesterol transport protein with expanding role in cell biology. *Science*. 1988;240:622–630.
4. Mazzone T. Apolipoprotein E secretion by macrophages: its potential physiological functions. *Curr Opin Lipidol*. 1996;7:303–307.
5. Beisiegel U. Receptors for triglyceride-rich lipoproteins and their role in lipoprotein metabolism. *Curr Opin Lipidol*. 1995;6:117–122.
6. Tsukamoto K, Tangirala R, Chun SH, Pure E, Rader DJ. Rapid regression of atherosclerosis induced by liver-directed gene transfer of apoE in apoE-deficient mice. *Arterioscler Thromb Vasc Biol*. 1999;19:2162–2170.
7. Tsukamoto K, Tangirala RK, Chun S, Usher D, Pure E, Rader DJ. Hepatic expression of apolipoprotein E inhibits progression of atherosclerosis without reducing cholesterol levels in LDL receptor-deficient mice. *Mol Ther*. 2000;1:189–194.
8. Bellosta S, Mahley RW, Sanan DA, Murata J, Newland DL, Taylor JM, Pitas RE. Macrophage-specific expression of human apolipoprotein E reduces atherosclerosis in hypercholesterolemic apolipoprotein E-null mice. *J Clin Invest*. 1995;96:2170–2179.
9. Fazio S, Babaev VR, Murray AB, Hasty AH, Carter KJ, Gleaves LA, Atkinson JB, Linton MF. Increased atherosclerosis in mice reconstituted with apolipoprotein E null macrophages. *Proc Natl Acad Sci U S A*. 1997;94:4647–4652.
10. Shimano H, Ohsuga J, Shimada M, Namba Y, Gotoda T, Harada K, Katsuki M, Yazaki Y, Yamada N. Inhibition of diet-induced atheroma formation in transgenic mice expressing apolipoprotein E in the arterial wall. *J Clin Invest*. 1995;95:469–476.
11. Gregg RE, Zech LA, Schaefer EJ, Brewer HB Jr. Type III hyperlipoproteinemia: defective metabolism of an abnormal apolipoprotein E. *Science*. 1981;211:584–586.
12. Weisgraber KH, Innerarity TL, Mahley RW. Abnormal lipoprotein receptor-binding activity of the human E apoprotein due to cysteine-arginine interchange at a single site. *J Biol Chem*. 1982;257:2518–2521.
13. Gregg RE, Zech LA, Schaefer EJ, Stark D, Wilson D, Brewer HB Jr. Abnormal in vivo metabolism of apolipoprotein E4 in humans. *J Clin Invest*. 1986;78:815–821.
14. Tsukamoto K, Smith P, Glick JM, Rader DJ. Liver-directed gene transfer and prolonged expression of three major human apoE isoforms in apoE-deficient mice. *J Clin Invest*. 1997;100:107–114.
15. Davignon J, Gregg RE, Sing CF. Apolipoprotein E polymorphism and atherosclerosis. *Arteriosclerosis*. 1988;8:1–21.
16. Wilson PW, Myers RH, Larson MG, Ordovas JM, Wolf PA, Schaefer EJ. Apolipoprotein E alleles, dyslipidemia, and coronary heart disease: the Framingham Offspring Study. *JAMA*. 1994;272:1666–1671.
17. Cullen P, Cignarella A, Brennhausen B, Mohr S, Assmann G, von Eckardstein A. Phenotype-dependent differences in apolipoprotein E metabolism and in cholesterol homeostasis in human monocyte-derived macrophages. *J Clin Invest*. 1998;101:1670–1677.
18. Smith JD, Miyata M, Ginsberg M, Grigaux C, Shmookler E, Plump AS. Cyclic AMP induces apolipoprotein E binding activity and promotes cholesterol efflux from a macrophage cell line to apolipoprotein acceptors. *J Biol Chem*. 1996;271:30647–30655.
19. Carey DJ, Rafferty CM, Todd MS. Effects of inhibition of proteoglycan synthesis on the differentiation of cultured rat Schwann cells. *J Cell Biol*. 1987;105:1013–1021.
20. Shimada K, Ozawa T. Modulation of glycosaminoglycan production and antithrombin III binding by cultured aortic endothelial cells treated with 4-methylumbelliferyl-β-D-xyloside. *Arteriosclerosis*. 1987;7:627–636.
21. Lucas M, Mazzone T. Cell surface proteoglycans modulate net synthesis and secretion of macrophage apolipoprotein E. *J Biol Chem*. 1996;271:13454–13460.
22. Obunike JC, Pillarisetti S, Paka L, Kako Y, Butteri MJ, Ho YY, Wagner WD, Yamada N, Mazzone T, Deckelbaum RJ, Goldberg IJ. The heparin-binding proteins apolipoprotein E and lipoprotein lipase enhance cellular proteoglycan production. *Arterioscler Thromb Vasc Biol*. 2000;20:111–118.
23. Lin CY, Huang ZH, Mazzone T. Interaction with proteoglycans enhances the sterol efflux produced by endogenous expression of macrophage apoE. *J Lipid Res*. 2001;42:1125–1133.
24. Murakami M, Horiuchi S, Takata K, Morino Y. Distinction in the mode of receptor-mediated endocytosis between high density lipoprotein and acetylated high density lipoprotein: evidence for high density lipoprotein receptor-mediated cholesterol transfer. *J Biochem (Tokyo)*. 1987;101:729–741.
25. Wickham TJ, Mathias P, Cheresh DA, Nemerow GR. Integrins αvβ3 and αvβ5 promote adenovirus internalization but not virus attachment. *Cell*. 1993;73:309–319.
26. Bergelson JM, Cunningham JA, Droguett G, Kurt-Jones EA, Krithivas A, Hong JS, Horwitz MS, Crowell RL, Finberg RW. Isolation of a common receptor for Coxsackie B viruses and adenoviruses 2 and 5. *Science*. 1997;275:1320–1323.
27. Von Eckardstein A, Langer C, Engel T, Schaukal I, Cignarella A, Reinhardt J, Lorkowski S, Li Z, Zhou X, Cullen P, Assmann G. ATP binding cassette transporter ABCA1 modulates the secretion of apolipoprotein E from human monocyte-derived macrophages. *FASEB J*. 2001;15:1555–1561.
28. Ji ZS, Pitas RE, Mahley RW. Differential cellular accumulation/retention of apolipoprotein E mediated by cell surface heparan sulfate proteoglycans: apolipoproteins E3 and E2 greater than E4. *J Biol Chem*. 1998;273:13452–13460.
29. Zhao Y, Mazzone T. LDL receptor binds newly synthesized apoE in macrophages: a precursor pool for apoE secretion. *J Lipid Res*. 1999;40:1029–1035.
30. Mahley RW, Huang Y, Rall SC Jr. Pathogenesis of type III hyperlipoproteinemia (dysbetalipoproteinemia): questions, quandaries, and paradoxes. *J Lipid Res*. 1999;40:1933–1949.
31. Ishigami M, Swertfeger DK, Granholm NA, Hui DY. Apolipoprotein E inhibits platelet-derived growth factor-induced vascular smooth muscle cell migration and proliferation by suppressing signal transduction and preventing cell entry to G1 phase. *J Biol Chem*. 1998;273:20156–20161.
32. Miyata M, Smith JD. Apolipoprotein E allele-specific antioxidant activity and effects on cytotoxicity by oxidative insults and β-amyloid peptides. *Nat Genet*. 1996;14:55–61.
33. Riddell DR, Graham A, Owen JS. Apolipoprotein E inhibits platelet aggregation through the L-arginine:nitric oxide pathway: implications for vascular disease. *J Biol Chem*. 1997;272:89–95.
34. Kelly ME, Clay MA, Mistry MJ, Hsieh-Li HM, Harmony JA. Apolipoprotein E inhibition of proliferation of mitogen-activated T lymphocytes: production of interleukin 2 with reduced biological activity. *Cell Immunol*. 1994;159:124–139.
35. Nathan BP, Bellosta S, Sanan DA, Weisgraber KH, Mahley RW, Pitas RE. Differential effects of apolipoproteins E3 and E4 on neuronal growth in vitro. *Science*. 1994;264:850–852.
36. van Bockxmeer FM, Mamotte CD, Gibbons FR, Taylor RR. Apolipoprotein ε4 homozygosity: a determinant of restenosis after coronary angioplasty. *Atherosclerosis*. 1994;110:195–202.
37. van Bockxmeer FM, Mamotte CD, Gibbons FA, Burke V, Taylor RR. Angiotensin-converting enzyme and apolipoprotein E genotypes and restenosis after coronary angioplasty. *Circulation*. 1995;92:2066–2071.

Association Between Insulin Resistance and Carotid Arteriosclerosis in Subjects With Normal Fasting Glucose and Normal Glucose Tolerance

Nobukazu Ishizaka, Yuko Ishizaka, Eiko Takahashi, Tadao Unuma, Ei-ichi Tooda, Ryozo Nagai, Masako Togo, Kazuhisa Tsukamoto, Hideki Hashimoto, Minoru Yamakado

Objective—We examined the possible association between insulin resistance and carotid arteriosclerosis in subjects who had both normal fasting glucose and normal glucose tolerance after intake of a glucose load.

Methods and Results—Our subjects were individuals who underwent general health screening at our institute, which included carotid ultrasound and oral glucose tolerance testing. Of the 1238 subjects enrolled in our study, 738 (60%) were classified as normal, defined as a normal fasting glucose level and normal glucose tolerance, and 334 (27%) and 166 (13%) were classified as borderline and diabetic, respectively, according to the criteria of the Japan Diabetes Society. The homeostasis model assessment of insulin resistance (HOMA-IR) was used as the index to measure insulin resistance. In normal-type subjects, univariate analysis showed that insulin resistance, but not insulin secretion, was associated with the presence of carotid plaque. Multivariate analysis showed that HOMA-IR was positively associated with carotid plaque in normal-type subjects, with an odds ratio of 1.19 (95% confidence interval, 1.00 to 1.41; $P<0.05$).

Conclusions—These data suggest the possibility that the presence of higher insulin resistance could be a risk factor for carotid arteriosclerosis in subjects with normal fasting glucose and normal glucose tolerance. (*Arterioscler Thromb Vasc Biol.* **2003;23:295-301.**)

Key Words: carotid ultrasound ■ atherosclerosis ■ diabetes ■ insulin resistance ■ risk factor

Several prospective epidemiological studies have suggested that there may be an association between insulin resistance and/or hyperinsulinemia and subsequent cardiovascular disease and stroke.[1-5] Furthermore, some studies have reported an association between insulin resistance and early carotid arteriosclerotic lesions,[6,7] the development of which is a known risk factor for myocardial infarction and stroke.[8] In interpreting these data, one needs to exercise caution, because an observed association may be dependent on other well-known atherogenic risk factors, such as other metabolic and hemodynamic disorders that may cluster in the subjects with increased insulin resistance and that compose the insulin-resistance syndrome.[9] Indeed, a large cross-sectional, population-based study in Sweden suggested that the association between insulin resistance in nondiabetic subjects and atherosclerosis was explained by its covariance with established risk factors.[9]

Patients with impaired glucose tolerance who may have features of the insulin resistance syndrome,[10] as well as diabetes, are at increased risk for developing atherosclerosis.[11,12] A recent study showed that subjects with impaired glucose tolerance had a risk of carotid stenosis 3-fold higher than did subjects with normal glucose tolerance, even after adjustment for several confounding risk factors.[13] Therefore, we wanted to know whether we could isolate subjects at high risk for developing atherosclerotic complications, not from nondiabetic subjects but from subjects evan without impaired glucose tolerance. To date, there has been little published information concerning whether increased insulin resistance is an independent risk factor for atherosclerotic diseases in subjects with both normal fasting glucose levels and normal glucose tolerance. The purpose of this study was to determine whether there was a possible association between insulin resistance and carotid arteriosclerosis by analyzing the population-based, cross-sectional data of these subjects.

Methods

Subjects

Between August 1994 and April 1999, 1238 subjects underwent general health screening tests at the Center for Multiphasic Health Testing and Services, Mitsui Memorial Hospital, which included both high-resolution B-mode carotid ultrasound and oral glucose tolerance testing. In Japan, regular health checkups for employees are legally mandated. Therefore, the majority of these subjects did

Received September 26, 2002; revision accepted November 20, 2002.

From the Departments of Cardiovascular Medicine (N.I., R.N.) and Metabolic Diseases (M.T., K.T.), University of Tokyo Graduate School of Medicine, the Center for Multiphasic Health Testing and Services, Mitsui Memorial Hospital (Y.I., E. Takahashi, T.U., E. Tooda, M.Y.), and Department of Hygiene and Public Health (H.H.), Teikyo University School of Medicine, Tokyo, Japan.

Correspondence to Nobukazu Ishizaka, MD, PhD, Department of Cardiovascular Medicine, University of Tokyo, Graduate School of Medicine, Hongo 7-3-1, Bunkyo-ku, Tokyo 113-8655, Japan. E-mail nobuishizka-tky@umin.ac.jp

Arterioscler Thromb Vasc Biol. **is available at http://www.atvbaha.org** **DOI: 10.1161/01.ATV.0000050142.09911.0B**

not have serious health problems. Within this study period, a total of 16 383 subjects underwent general health screening at our institute, and only 8% (1238) of these underwent general health screening that included both high-resolution B-mode carotid ultrasound and oral glucose tolerance testing; these individuals make up the study population of the present work. The enrolled subjects were significantly older, had a significantly higher body mass index (BMI), and were more likely to be men, compared with the total population (data not shown). Therefore, it could be said that there was some selection bias when the participant was scheduled to undergo carotid ultrasonography together with oral glucose testing, though, it was neither the decision nor recommendation by the physicians.

Carotid Ultrasound

Carotid artery status was studied with a high-resolution, B-mode ultrasound system (Sonolayer SSA270A, Toshiba) equipped with a 7.5-MHz transducer (PLF-703ST, Toshiba). The carotid arteries were examined bilaterally at the levels of the common carotid artery, the bifurcation, and the internal carotid arteries from transverse and longitudinal orientations by trained sonographers. The intima-media thickness was measured by a computer-assisted method by experienced sonographers who were unaware of the subjects' clinical and laboratory findings. Plaque was defined as a clearly isolated focal thickening of the intima-media layer with a thickness ≥1.3 mm at the common or internal carotid artery or the carotid bulb. Carotid wall thickening was judged to be present when the intima-media thickness, which was measured at the far wall of the distal 10 mm of the common carotid artery, was ≥1.0 mm.

Glucose Tolerance Test and Classification of the Subjects

No subjects in the present study were being treated with either oral medications or insulin for diabetes. All subjects underwent an oral 75-g glucose tolerance test, for which their levels of plasma glucose and serum insulin were measured before administration of the glucose load and 30, 60, and 120 minutes later. With the data obtained during the test, subjects were classified into 1 of 3 categories according to the criteria of the Committee for the Classification and Diagnosis of Diabetes Mellitus of the Japan Diabetes Society.[14] Normal-type subjects were defined as having a fasting plasma glucose (FPG) <110 mg/dL (<6.1 mmol/L) and a 2-hour plasma glucose <140 mg/dL (<7.8 mmol/L), whereas diabetic-type subjects were defined as having an FPG ≥126 mg/dL (≥7.0 mmol/L) and/or a 2-hour plasma glucose ≥200 mg/dL (≥11.1 mmol/L). Borderline-type subjects included those who were of neither the diabetic nor normal type. Normal-type subjects met the criteria of having normal fasting glucose (NFG)[15] and normal glucose tolerance (NGT),[16] whereas borderline-type subjects included those with both impaired fasting glucose[15] and impaired glucose tolerance.[16]

Risk Factors

BMI was calculated as weight (kg)/height (m^2). Subjects were said to be hypertensive if they had a systolic blood pressure ≥140 mm Hg, a diastolic blood pressure of ≥90 mm Hg, or both.

Laboratory Tests

Blood samples were taken from our subjects after an overnight fast. Total cholesterol (TC), HDL cholesterol (HDL-C), and triglycerides (TGs) were determined enzymatically, and hemoglobin A_{1C} was determined by a latex agglutination immunoassay. The subjects' homeostasis model assessment of insulin resistance (HOMA-IR), which is a measure of the degree of their insulin resistance, was calculated as [fasting insulin (μU/mL)×fasting glucose (mg/dL)]/405.[17] The correlation coefficient of HOMA-IR versus fasting insulin in normal-type subjects was 0.993. The insulinogenic index, an index of early-phase insulin secretion and thus, beta cell function, was defined as the ratio of the increment of serum insulin to that of plasma glucose 30 minutes after a glucose load, ie, (Δinsulin 0 to 30 minutes)/(Δplasma glucose 0 to 30 minutes), which was expressed in (μU/mL)/(mg/dL).

Statistical Analysis

The χ^2 test, ANOVA, and univariate and multivariate logistic regression analyses performed with Statistica version 5J and StatView version 5.0 software, were used to analyze the data in this study. Age, BMI, TC, HDL-C, TGs, and hemoglobin A_{1C} were included as continuous variables, and others were included as categorical variables. Statistical significance was taken at $P<0.05$. Results were expressed as the mean±SD unless otherwise stated.

Results

Study Subjects

Of the 1238 participants in this study, 738 (60%) were normal-type, 334 (27%) were borderline type, and 166 (13%) were diabetic-type subjects. The baseline characteristics and laboratory data for each group are shown in Table 1. The mean age in the normal-type, borderline-type, and diabetic type subjects were 57.4 (24 to 82), 59.2 (24 to 88), and 60.0 years (27 to 79 years), respectively. HOMA-IR was lowest in normal-type subjects, with a range of 0.50 to 8.07 (median, 1.25), followed by borderline-type subjects, with a range of 0.62 to 12.4 (median, 1.96), and was highest in diabetic-type subjects, with a range of 0.71 to 11.1 (median, 2.78). The insulinogenic index was highest in normal-type subjects, followed by borderline-type subjects and then diabetic-type subjects. Carotid plaque was present in 22%, 28%, and 30% of normal-type, borderline-type, and diabetic-type subjects, respectively ($P<0.05$ by χ^2 test). Carotid intima-media thickness was the smallest in the normal-type subjects, followed successively by borderline-type and diabetic-type subjects, but these differences did not reach statistical significance. The prevalence of carotid artery wall thickening (intima-media thickness ≥1.0 mm) in normal-type, borderline-type, and diabetic-type subjects was 14%, 16%, and 20%, respectively (NS by χ^2 test).

Univariate Analyses Examining the Association Between Insulin Resistance and Carotid Plaque

Results of the univariate analysis are shown in Table 2. Hemoglobin A_{1C}, but not fasting glucose, was associated with carotid plaque in normal-type subjects. HOMA-IR was positively associated with carotid plaque in the population as a whole, as well as in the normal-type subjects, with odds ratios of 1.12 (95% confidence interval, 1.03 to 1.21, $P<0.01$) and 1.21 (95% confidence interval, 1.04 to 1.41, $P=0.014$), respectively. In contrast, the insulinogenic index was not significantly associated with carotid plaque in either the entire group of subjects as a whole or in normal-type subjects. A similar analysis was performed to assess the possible association between HOMA-IR and carotid intima-media thickening; however, there was no significant association between these variables in either the group as a whole or in normal-type subjects (Table 3).

Relation Between Insulin Resistance and Atherogenic Risk Factors in Normal-Type Subjects

Before performing multivariate analyses, we assessed the relation between HOMA-IR and atherogenic risk factors in normal-type subjects. HOMA-IR showed weak but positive correlations with systolic blood pressure (0.26, $P<0.0001$), TC (0.07, $P<0.05$), and TGs (0.19, $P<0.0001$) and a nega-

TABLE 1. Baseline Characteristics

	All (n=1238)	Normal (n=738)	Borderline (n=334)	Diabetic (n=166)	P
Clinical characteristics					
Age, y	58.2±10.1	57.4±10.5	59.2±9.8	60.0±8.5	0.0042
Sex, female/male	329/909	260/478	53/281	16/150	<0.0001
BMI, kg/m^2	23.6±3.1	23.0±2.9	24.4±3.0	24.7±3.3	<0.0001
Systolic blood pressure, mm Hg	128±21	123±19	134±20	137±23	<0.0001
Diastolic blood pressure, mm Hg	78±13	75±12	82±13	83±14	<0.0001
Hypertension, %	341 (27)	146 (20)	121 (36)	74 (45)	<0.0001
Never smoker, %	484 (39)	338 (46)	104 (31)	42 (25)	0.0050
Current smoker, %	506 (41)	279 (38)	142 (43)	85 (51)	0.0004
Ex-smoker, %	248 (20)	121 (16)	88 (26)	39 (23)	<0.0001
Laboratory data					
Lipid metabolism					
Total cholesterol, mmol/L	5.4±0.9	5.4±0.9	5.4±0.9	5.3±0.8	0.72
Triglycerides, mmol/L	1.6±1.2	1.3±0.9	1.9±1.3	2.1±1.4	<0.0001
HDL-cholesterol, mmol/L	1.4±0.4	1.5±0.5	1.3±0.4	1.2±0.3	<0.0001
Glucose metabolism					
Fasting glucose, mmol/L	5.9±1.2	5.3±0.4	6.0±0.5	8.0±1.9	<0.0001
30-min glucose, mmol/L	9.3±2.3	8.2±1.5	9.8±1.5	12.9±2.7	<0.0001
1-h glucose, mmol/L	9.5±3.7	7.5±2.1	10.7±2.3	15.8±3.5	<0.0001
2-h glucose, mmol/L	7.9±3.7	6.0±1.1	8.4±1.3	15.2±4.4	<0.0001
Fasting insulin, μU/mL	7.4±4.9	6.5±4.4	8.4±5.2	9.3±5.1	<0.0001
30-min insulin, μU/mL	41.3±30.2	43.8±30.1	44.2±32.9	24.4±15.7	<0.0001
1-h insulin, μU/mL	49.0±34.7	47.2±31.5	59.1±42.2	36.2±24.7	<0.0001
2-h insulin, μU/mL	42.1±30.1	33.3±19.3	59.3±40.4	46.2±30.5	<0.0001
Hemoglobin A_{1C}, %	5.3±0.7	5.1±0.4	5.3±0.4	6.5±1.1	<0.0001
HOMA-IR	1.98±1.50	1.57±1.20	2.26±1.42	3.38±2.09	<0.0001
Insulinogenic index (μU/mL per mg/dL)	0.67±1.01	0.80±1.20	0.60±0.60	0.22±0.51	<0.0001
Carotid ultrasonographic data					
Carotid plaque, %	305 (25)	160 (22)	95 (28)	50 (30)	0.013
Intima-media thickness, mm	0.78±0.45	0.76±0.48	0.80±0.45	0.82±0.25	0.24
Intima-media thickening	195 (16)	107 (14)	55 (16)	33 (20)	0.21

tive correlation with HDL-C (-0.17, $P<0.0001$) in this group. Notably, the correlation between HOMA-IR and hemoglobin A_{1C} was not statistically significant (0.036, $P=0.32$). Similarly, no statistically significant correlation was observed between the insulinogenic index and atherogenic risk factors, such as systolic blood pressure (0.027, $P=0.47$), TC (0.005, $P=0.89$), TG (−0.12, $P=0.74$), HDL-C (-0.059, $P=0.11$), and hemoglobin A_{1C} (0.045, $P=0.22$).

Multivariate Analyses of Insulin Resistance and Carotid Plaque

The association between HOMA-IR and carotid plaque was assessed by multivariate logistic regression analysis, which included the following variables: age, sex, systolic blood pressure, TC, HDL-C, TGs, hemoglobin A_{1C}, and smoking status (Table 4). In this model, HOMA-IR remained a significant and independent predictor of carotid plaque in normal-type subjects, with an odds ratio of 1.19 (95% confidence interval, 1.00 to 1.41, $P<0.05$). In contrast, HOMA-IR was not associated with carotid intima-media thickening (odds ratio, 1.01; 95% confidence interval, 0.87 to 1.30, $P=0.52$).

Discussion

In this study, we investigated whether there was an association between insulin resistance, assessed by HOMA-IR, and the presence of carotid plaque in normal-type subjects, defined as those who had both NFG and NGT. Univariate analysis showed that HOMA-IR and hemoglobin A_{1C} levels, but not fasting glucose, were positively associated with the presence of carotid plaque. Insulin resistance was found to be positively associated, though weakly, with blood pressure, TC, and TGs and negatively with HDL-C. Multivariate analysis with other confounding risk factors for atherosclerosis, including hemoglobin A_{1C}, demonstrated that HOMA-IR was also independently associated with the presence of carotid plaque, with an odds ratio of 1.19 (95% confidence interval, 1.00 to 1.41, $P<0.05$), indicating that the association

TABLE 2. Univariate Analysis For Carotid Plaque

	All		Normal		Borderline		Diabetic	
	Odds Ratio (95% CI)	*P*	Odds Ratio (95% CI)	*P*	Odds Ratio (95% CI)	*P*	Odds Ratio (95% CI)	*P*
Male sex	2.45 (1.735–3.48)	<0.00001	2.86 (1.85–4.447)	<0.00001	1.86 (0.88–3.94)	0.1	0.69 (0.23–2.06)	0.5
Age, per y	1.11 (1.09–1.13)	<0.00001	1.11 (1.09–1.14)	<0.00001	1.09 (1.06–1.13)	<0.00001	1.10 (1.05–1.15)	0.00008
BMI, per 1 kg/m^2	1.05 (1.01–1.09)	0.034	1.08 (1.02–1.15)	0.01	1.00 (0.93–1.09)	0.95	0.94 (0.84–1.05)	0.28
Systolic blood pressure, per 1 mm Hg	1.02 (1.01–1.03)	<0.00001	1.02 (1.01–1.03)	0.00057	1.07 (1.02–1.11)	0.0015	1.02 (1.00–1.03)	0.024
Total cholesterol, per 1 mmol/L	1.12 (0.97–1.30)	0.12	1.16 (0.96–1.39)	0.12	0.97 (0.73–1.29)	0.84	1.37 (0.89–2.10)	0.14
HDL cholesterol, per 1 mmol/L	0.63 (0.46–0.87)	0.0047	0.99 (0.97–1.00)	0.01	0.90 (0.50–1.62)	0.72	0.86 (0.31–2.39)	0.8
Triglycerides, per 1 mmol/L	1.09 (0.980–1.22)	0.097	1.22 (1.03–1.45)	0.018	0.89 (0.72–1.10)	0.26	1.02 (0.79–1.30)	0.86
Fasting plasma glucose, per 1 mg/dL	1.00 (1.00–1.01)	0.16	1.01 (0.99–1.04)	0.34	0.99 (0.97–1.02)	0.57	1.00 (0.99–1.01)	0.42
Hemoglobin A_{1c}, per 1%	1.34 (1.13–1.58)	0.00065	2.70 (1.68–4.33)	0.00003	1.59 (0.90–2.79)	0.1	0.96 (0.70–1.30)	0.78
Fasting insulin	1.04 (1.01–1.06)	0.005	1.04 (1.01–1.09)	0.02	1.00 (0.96–1.06)	0.68	1.02 (0.96–1.09)	0.45
HOMA-IR, per 1	1.12 (1.03–1.21)	0.0075	1.21 (1.04–1.41)	0.014	1.03 (0.87–1.22)	0.74	1.00 (0.85–1.17)	0.96
Insulinogenic index, per 1	0.96 (0.84–1.10)	0.58	1.02 (0.88–1.19)	0.76	0.89 (0.57–1.38)	0.59	0.65 (0.15–2.77)	0.55
Current smoker*	1.51 (1.11–2.06)	0.0068	1.50 (1.00–2.24)	0.046	1.12 (0.62–2.00)	0.7	2.09 (0.84–5.19)	0.11
Ex-smoker*	1.93 (1.35–2.76)	0.00025	2.04 (1.25–3.34)	0.0037	1.33 (0.70–2.52)	0.37	2.38 (0.85–6.67)	0.094

*Never smoker was used as reference.

between insulin resistance and carotid atherosclerosis was independent of other atherogenic risk factors.

Although HOMA-IR, calculated with fasting glucose and fasting insulin levels, was used to assess the degree of insulin resistance in our subjects, the estimation of insulin resistance by this approach may be somewhat less accurate compared with the use of glucose clamping. However, it is not feasible to perform glucose clamp studies in the general health screening setting. Furthermore, there has been shown to be good agreement between HOMA-IR and clamp-measured glucose disposal in subjects with various degree of glucose tolerance.[18] Therefore, HOMA-IR was considered a useful model for assessing insulin resistance in epidemiological studies[18] such as ours.

The prevalence of subjects with borderline-type (27%) and diabetic-type (13%) glucose metabolism in this study was somewhat higher than expected. This may be due, at least in part, to the reduction in FPG threshold used to screen for

TABLE 3. Univariate Analysis For Carotid Intima-Media Thickening

	All		Normal		Borderline		Diabetic	
	Odds Ratio (95% CI)	*P*	Odds Ratio (95% CI)	*P*	Odds Ratio (95% CI)	*P*	Odds Ratio (95% CI)	*P*
Male sex	1.79 (1.21–2.67)	0.0034	2.07 (1.26–3.38)	0.0033	0.96 (0.43–2.12)	0.91	1.82 (0.38–8.72)	0.44
Age, per y	1.08 (1.06–1.10)	<0.00001	1.11 (1.08–1.13)	<0.00001	1.05 (1.01–1.08)	0.005	1.03 (0.99–1.08)	0.15
BMI, per 1 kg/m^2	1.02 (0.97–1.07)	0.44	1.03 (0.96–1.11)	0.37	1.01 (0.92–1.11)	0.86	0.95 (0.84–1.08)	0.43
Systolic blood pressure, per 1 mm Hg	1.01 (1.01–1.02)	0.00046	1.02 (1.01–1.03)	0.00076	1.00 (0.98–1.01)	0.64	1.02 (1.00–1.03)	0.04
Total cholesterol, per 1 mmol/L	1.04 (0.87–1.23)	0.69	1.01 (0.80–1.27)	0.94	1.20 (0.85–1.69)	0.3	0.90 (1.49–0.55)	0.69
HDL cholesterol, per 1 mmol/L	0.52 (0.35–0.78)	0.0012	0.52 (0.31–0.88)	0.012	0.71 (0.34–1.49)	0.36	0.36 (0.10–1.33)	0.12
Triglycerides, per 1 mmol/L	1.02 (0.89–1.16)	0.78	1.03 (0.83–1.27)	0.78	0.93 (0.73–1.19)	0.57	1.00 (0.74–1.65)	0.99
Fasting plasma glucose, per 1 mg/dL	1.01 (1.00–1.01)	0.063	1.04 (1.01–1.07)	0.015	1.01 (0.98–1.04)	0.54	1.00 (0.99–1.01)	0.79
Hemoglobin A_{1c}, per 1%	1.06 (0.60–1.30)	0.59	0.76 (0.45–1.31)	0.32	0.60 (0.30–1.17)	0.13	1.10 (0.78–1.55)	0.58
Fasting insulin	1.04 (1.01–1.06)	0.005	1.04 (1.01–1.09)	0.02	1.01 (0.96–1.06)	0.68	1.02 (0.96–1.09)	0.45
HOMA-IR, per 1	1.06 (0.96–1.17)	0.23	1.10 (0.93–1.30)	0.25	0.97 (0.79–1.21)	0.8	0.99 (0.82–1.20)	0.93
Insulinogenic index, per 1	0.94 (0.80–1.11)	0.48	1.02 (0.86–1.21)	0.82	0.61 (0.30–1.22)	0.15	0.40 (0.03–5.24)	0.48
Current smoker*	1.12 (0.78–1.60)	0.54	1.09 (0.68–1.74)	0.73	0.61 (0.27–1.35)	0.21	4.00 (1.09–14.7)	0.035
Ex-smoker*	1.61 (1.07–2.42)	0.02	1.65 (0.95–2.89)	0.072	1.00 (0.34–2.96)	0.99	4.48 (1.10–18.3)	0.034

*Never smoker was used as reference.

TABLE 4. Multivariate Analysis For Carotid Plaque

	Odds Ratio (95% CI)	P
Male sex	1.79 (0.98–3.28)	0.055
Age, per y	1.12 (1.09–1.15)	<0.00001
Systolic blood pressure, per 1 mm Hg	1.00 (0.99–1.01)	0.99
Total cholesterol, per 1 mmol/L	1.25 (0.98–1.61)	0.072
HDL cholesterol, per 1 mmol/L	0.88 (0.50–1.54)	0.64
Triglycerides, per 1 mmol/L	1.21 (0.95–1.55)	0.11
Hemoglobin A1C, per 1%	1.82 (1.04–3.19)	0.032
HOMA-IR, per 1	1.19 (1.00–1.41)	0.045
Current smoker*	1.67 (0.98–2.85)	0.057
Ex-smoker*	1.44 (0.77–2.70)	0.24

*Never smoker was used as reference.

diabetes mellitus, from 7.8 to 7.0 mmol/L according to the American Diabetes Association,[16] which may result in a >2-fold increase in the number of newly diagnosed diabetic subjects.[19] Indeed, using the same criteria as in our study, Liao et al[20] showed that of 562 Japanese-Americans in King County, Washington, the number of the subjects with normal-type, borderline-type, and diabetic-type responses were 307 (55%), 212 (38%), and 77 (14%), respectively, which was similar to the distribution seen in our study population. When interpreting our data, which suggest that there is an association between insulin resistance and atherosclerosis, we need to exercise caution for 2 reasons. First, other metabolic and hemodynamic disorders included in the insulin resistance syndrome may cluster in subjects with increased insulin resistance,[9] making it difficult to assess the independent association between insulin resistance and arteriosclerotic diseases. Second, HOMA-IR provides useful information only when this parameter can predict a higher incidence of arteriosclerotic diseases independent of other factors such as plasma glucose and hemoglobin A_{1C}. In our study, as in a previous report,[21] plasma glucose was not a predictor of carotid plaque. Furthermore, there was no statistically significant relation between hemoglobin A_{1C} and HOMA-IR levels in normal-type subjects, both of which were independently associated with carotid plaque.

In this study, we assessed the possible association between insulin resistance, carotid plaque, and carotid-media thickening. There have been several previous reports in which the association between carotid intima-media thickness and insulin resistance has been investigated in a nondiabetic population. Some studies showed a lack of independent association between insulin resistance and carotid arteriosclerosis,[9,22,23] whereas others showed a positive association between these variables.[24] Snehalatha et al[22] reported lack of an association between insulin resistance and carotid intima-media thickness in nondiabetic Asian subjects. Bonora et al[23] reported that carotid intima-media thickness was associated with insulin resistance in nondiabetic subjects, as determined by univariate analysis, but was not associated by multivariate analysis, although their number of enrolled subjects (n=58) was relatively small. Hedblad et al[9] showed that the association between insulin resistance and carotid intima-media thickness in nondiabetic subjects and atherosclerosis was explained by its covariance with established risk factors. Although the target populations were different from those of our study (our subjects were limited to those who had both NFG and NGT, whereas nondiabetic subjects enrolled in the aforementioned studies may have included not only subjects in this category but also subjects with impaired fasting glucose or impaired glucose tolerance), similar results were obtained. On the other hand, some studies have shown an independent association between carotid intima-media thickness and insulin resistance. De Pergola et al[24] reported an independent association between insulin sensitivity and the thickness of the intima-media complex after adjusting the data for age, BMI, waist circumference, mean blood pressure levels, and plasma glucose and lipids. Similarly, Shinozaki et al[25] and Suzuki et al[26] reported that insulin resistance was independently and statistically significantly associated with carotid intima-media thickness in nondiabetic subjects. The conclusions of these 3 articles, which differ from ours, may be partially explained by the fact that the their target populations were nondiabetic subjects and thus, may have included subjects with impaired glucose tolerance and/or increased fasting glucose; in addition, the latter 2 studies examined the relation between carotid intima-media thickness and insulin resistance in a subpopulation of subjects with vasospastic angina and essential hypertension, respectively.

Few articles have examined the possible relation between carotid plaque and insulin resistance with a study population limited to nondiabetic subjects. Shinozaki et al[25] reported that carotid plaque, which had been defined as a distinct area with >50% intima-media thickness than neighboring sites (usually >1.2 mm) in subjects with vasospastic angina was statistically significantly associated with insulin resistance. Although subjects with impaired glucose tolerance were also included in their study population, they reached a conclusion similar to ours.

It has been reported that increases in intima-media thickness are related to locally detected atherosclerotic plaque.[27] One may wonder why HOMA-IR was associated with carotid plaque but not with carotid intima-media thickness in normal-type subjects. A recent study in Japan found that the prevalence of intima-media thickness and plaque were not associated in very old (>90 years of age) subjects,[28] which suggests the possibility that carotid intima-media thickening and plaque may have some distinct pathophysiological features. In addition, the prevalence of carotid plaque has been reported to be higher than that of intima-media thickening in some studies, which may further support the notion that carotid intima-media thickening is not just a less-severe lesion of carotid plaque. We do not know the exact reason why HOMA-IR was associated with only carotid plaque, but a possible explanation may be that different risk factors may affect only carotid plaque or carotid intima-media thickness if the pathological features differ, at least in part, between these 2 conditions. Indeed, in our study population, multivariate analysis showed that blood pressure and serum levels of TC were associated with carotid plaque but not with carotid intima-media thickening.

Both insulin resistance[29,30] and diminished insulin section[31,32] are known to predict the future development of

diabetes. Recently, it has become possible to treat patients in the clinical setting with insulin-sensitizing drugs. Our data and those of others[33] suggest that insulin sensitization, rather than the promotion of insulin secretion, would be the better therapeutic strategy in light of the fact that elevated insulin levels could cluster with other atherogenic risk factors, and insulin resistance itself is also an independent risk factor for the development of carotid arteriosclerosis. Because ours was not a longitudinal study, we cannot predict what percentage of our normal-type subjects will go on to develop diabetes later in life. Whether administration of insulin-sensitizing drugs, as opposed to insulin secretagogues, to prediabetic and diabetic individuals can prevent atherogenic complications remains to be investigated in longitudinal, double-blind studies. Because insulin resistance as well as levels of TGs and HDL-C may be related to the size of LDL, which has been reported to be associated with carotid and femoral arteries,[34] the relation between HOMA-IR and carotid plaque observed in the present study may be explained by variations in the sizes of LDL particles. This possibility should also be clarified in future studies.

An increase in systolic blood pressure was found to be a risk factor for carotid plaque in normal-type subjects by univariate analysis but not by multivariate analysis in our study. On the other hand, we found that each 10 mm Hg increase in systolic blood pressure in borderline-type or diabetic-type subjects was associated with a 20% increase in carotid plaque ($P=0.0012$). These findings suggest that control of blood pressure is 1 of the potentially modifiable risk factors for the development of arteriosclerosis in subjects with abnormal glucose metabolism, a similar conclusion that has been reached in the recent UK Prospective Diabetes Study.[35]

In conclusion, analysis of cross-sectional data obtained from subjects undergoing general health screening tests showed that insulin resistance, calculated as HOMA-IR, was positively associated with carotid plaque formation in subjects who showed both NFG and NGT. This association remained significant even when other atherogenic risk factors, including hemoglobin A_{1C} levels, were factored in as covariates. Thus, HOMA-IR may be a useful index to predict carotid plaque formation in the subjects with both NFG and NGT.

References

1. Fontbonne AM, Eschwege EM. Insulin and cardiovascular disease: Paris Prospective Study. *Diabetes Care*. 1991;14:461–469.
2. Welborn TA, Wearne K. Coronary heart disease incidence and cardiovascular mortality in Busselton with reference to glucose and insulin concentrations. *Diabetes Care*. 1979;2:154–160.
3. Despres JP, Lamarche B, Mauriege P, Cantin B, Dagenais GR, Moorjani S, Lupien PJ. Hyperinsulinemia as an independent risk factor for ischemic heart disease. *N Engl J Med*. 1996;334:952–957.
4. Pyorala M, Miettinen H, Halonen P, Laakso M, Pyorala K. Insulin resistance syndrome predicts the risk of coronary heart disease and stroke in healthy middle-aged men: the 22-year follow-up results of the Helsinki Policemen Study. *Arterioscler Thromb Vasc Biol*. 2000;20:538–544.
5. Bonora E, Formentini G, Calcaterra F, Lombardi S, Marini F, Zenari L, Saggiani F, Poli M, Perbellini S, Raffaelli A, Cacciatori V, Santi L, Targher G, Bonadonna R, Muggeo M. HOMA-estimated insulin resistance is an independent predictor of cardiovascular disease in type 2 diabetic subjects: prospective data from the Verona Diabetes Complications Study. *Diabetes Care*. 2002;25:1135–1141.
6. Laakso M, Sarlund H, Salonen R, Suhonen M, Pyorala K, Salonen JT, Karhapaa P. Asymptomatic atherosclerosis and insulin resistance. *Arterioscler Thromb*. 1991;11:1068–1076.
7. Agewall S, Fagerberg B, Attvall S, Wendelhag I, Urbanavicius V, Wikstrand J. Carotid artery wall intima-media thickness is associated with insulin-mediated glucose disposal in men at high and low coronary risk. *Stroke*. 1995;26:956–960.
8. O'Leary DH, Polak JF, Kronmal RA, Manolio TA, Burke GL, Wolfson SK Jr. Carotid-artery intima and media thickness as a risk factor for myocardial infarction and stroke in older adults: Cardiovascular Health Study Collaborative Research Group. *N Engl J Med*. 1999;340:14–22.
9. Hedblad B, Nilsson P, Janzon L, Berglund G. Relation between insulin resistance and carotid intima-media thickness and stenosis in non-diabetic subjects: results from a cross-sectional study in Malmo, Sweden. *Diabet Med*. 2000;17:299–307.
10. Davies MJ, Raymond NT, Day JL, Hales CN, Burden AC. Impaired glucose tolerance and fasting hyperglycaemia have different characteristics. *Diabet Med*. 2000;17:433–440.
11. Tominaga M, Eguchi H, Manaka H, Igarashi K, Kato T, Sekikawa A. Impaired glucose tolerance is a risk factor for cardiovascular disease, but not impaired fasting glucose: the Funagata Diabetes Study. *Diabetes Care*. 1999;22:920–924.
12. Bonora E, Kiechl S, Oberhollenzer F, Egger G, Bonadonna RC, Muggeo M, Willeit J. Impaired glucose tolerance, type II diabetes mellitus and carotid atherosclerosis: prospective results from the Bruneck Study. *Diabetologia*. 2000;43:156–164.
13. Bonora E. Postprandial peaks as a risk factor for cardiovascular disease: epidemiological perspectives. *Int J Clin Pract Suppl*. 2002;129:5–11.
14. Kuzuya T, Nakagawa S, Satoh J, Kanazawa Y, Iwamoto Y, Kobayashi M, Nanjo K, Sasaki A, Seino Y, Ito C, Shima K, Nonaka K, Kadowaki T. Report of the committee on the classification and diagnostic criteria of diabetes mellitus. *Diabetes Res Clin Pract*. 2002;55:65–85.
15. Harris MI, Eastman RC, Cowie CC, Flegal KM, Eberhardt MS. Comparison of diabetes diagnostic categories in the US population according to the 1997 American Diabetes Association and 1980–1985 World Health Organization diagnostic criteria. *Diabetes Care*. 1997;20:1859–1862.
16. Alberti KG, Zimmet PZ. Definition, diagnosis and classification of diabetes mellitus and its complications. part 1: diagnosis and classification of diabetes mellitus provisional report of a WHO consultation. *Diabet Med*. 1998;15:539–553.
17. Matthews DR, Hosker JP, Rudenski AS, Naylor BA, Treacher DF, Turner RC. Homeostasis model assessment: insulin resistance and beta-cell function from fasting plasma glucose and insulin concentrations in man. *Diabetologia*. 1985;28:412–419.
18. Bonora E, Targher G, Alberiche M, Bonadonna RC, Saggiani F, Zenere MB, Monauni T, Muggeo M. Homeostasis model assessment closely mirrors the glucose clamp technique in the assessment of insulin sensitivity: studies in subjects with various degrees of glucose tolerance and insulin sensitivity. *Diabetes Care*. 2000;23:57–63.
19. Gourdy P, Ruidavets JB, Ferrieres J, Ducimetiere P, Amouyel P, Arveiler D, Cottel D, Lamamy N, Bingham A, Hanaire-Broutin H. Prevalence of type 2 diabetes and impaired fasting glucose in the middle-aged population of three French regions: the MONICA study 1995–97. *Diabetes Metab*. 2001;27:347–358.
20. Liao D, Shofer JB, Boyko EJ, McNeely MJ, Leonetti DL, Kahn SE, Fujimoto WY. Abnormal glucose tolerance and increased risk for cardiovascular disease in Japanese-Americans with normal fasting glucose. *Diabetes Care*. 2001;24:39–44.
21. Bonora E, Kiechl S, Willeit J, Oberhollenzer F, Egger G, Bonadonna R, Muggeo M. Plasma glucose within the normal range is not associated with carotid atherosclerosis: prospective results in subjects with normal glucose tolerance from the Bruneck Study. *Diabetes Care*. 1999;22:1339–1346.
22. Snehalatha C, Vijay V, Suresh MR, Satyavani K, Sivasankari S, Megha T, Radhika S, Ramachandran A. Lack of association of insulin resistance and carotid intimal medial thickness in non-diabetic Asian Indian subjects. *Diabetes Metab Res Rev*. 2001;17:444–447.
23. Bonora E, Tessari R, Micciolo R, Zenere M, Targher G, Padovani R, Falezza G, Muggeo M. Intimal-medial thickness of the carotid artery in nondiabetic and NIDDM patients: relationship with insulin resistance. *Diabetes Care*. 1997;20:627–631.
24. De Pergola G, Ciccone M, Pannacciulli N, Modugno M, Sciaraffia M, Minenna A, Rizzon P, Giorgino R. Lower insulin sensitivity as an independent risk factor for carotid wall thickening in normotensive, non-

diabetic, non-smoking normal weight and obese premenopausal women. *Int J Obes Relat Metab Disord.* 2000;24:825–829.
25. Shinozaki K, Hattori Y, Suzuki M, Hara Y, Kanazawa A, Takaki H, Tsushima M, Harano Y. Insulin resistance as an independent risk factor for carotid artery wall intima media thickening in vasospastic angina. *Arterioscler Thromb Vasc Biol.* 1997;17:3302–3310.
26. Suzuki M, Shinozaki K, Kanazawa A, Hara Y, Hattori Y, Tsushima M, Harano Y. Insulin resistance as an independent risk factor for carotid wall thickening. *Hypertension.* 1996;28:593–598.
27. Bonithon-Kopp C, Touboul PJ, Berr C, Leroux C, Mainard F, Courbon D, Ducimetiere P. Relation of intima-media thickness to atherosclerotic plaques in carotid arteries: the Vascular Aging (EVA) Study. *Arterioscler Thromb Vasc Biol.* 1996;16:310–316.
28. Homma S, Hirose N, Ishida H, Ishii T, Araki G. Carotid plaque and intima-media thickness assessed by B-mode ultrasonography in subjects ranging from young adults to centenarians. *Stroke.* 2001;32:830–835.
29. Sicree RA, Zimmet PZ, King HO, Coventry JS. Plasma insulin response among Nauruans: prediction of deterioration in glucose tolerance over 6 yr. *Diabetes.* 1987;36:179–186.
30. Haffner SM, Stern MP, Mitchell BD, Hazuda HP, Patterson JK. Incidence of type II diabetes in Mexican Americans predicted by fasting insulin and glucose levels, obesity, and body-fat distribution. *Diabetes.* 1990;39: 283–288.
31. Kadowaki T, Miyake Y, Hagura R, Akanuma Y, Kajinuma H, Kuzuya N, Takaku F, Kosaka K. Risk factors for worsening to diabetes in subjects with impaired glucose tolerance. *Diabetologia.* 1984;26:44–49.
32. Chen KW, Boyko EJ, Bergstrom RW, Leonetti DL, Newell-Morris L, Wahl PW, Fujimoto WY. Earlier appearance of impaired insulin secretion than of visceral adiposity in the pathogenesis of NIDDM: 5-year follow-up of initially nondiabetic Japanese-American men. *Diabetes Care.* 1995;18:747–753.
33. Haffner SM, Mykkanen L, Festa A, Burke JP, Stern MP. Insulin-resistant prediabetic subjects have more atherogenic risk factors than insulin-sensitive prediabetic subjects: implications for preventing coronary heart disease during the prediabetic state. *Circulation.* 2000;101:975–980.
34. Hulthe J, Bokemark L, Wikstrand J, Fagerberg B. The metabolic syndrome, LDL particle size, and atherosclerosis: the Atherosclerosis and Insulin Resistance (AIR) study. *Arterioscler Thromb Vasc Biol.* 2000;20: 2140–2147.
35. Adler AI, Stevens RJ, Neil A, Stratton IM, Boulton AJ, Holman RR. UKPDS 59: hyperglycemia and other potentially modifiable risk factors for peripheral vascular disease in type 2 diabetes. *Diabetes Care.* 2002; 25:894–899.

Am J Physiol Cell Physiol 284: C729–C737, 2003.
First published November 20, 2002; 10.1152/ajpcell.00166.2002.

Localization of Na^+-HCO_3^- cotransporter (NBC-1) variants in rat and human pancreas

HIROAKI SATOH,[1] NOBUO MORIYAMA,[2] CHIAKI HARA,[1] HIDEOMI YAMADA,[1] SHOKO HORITA,[1] MOTOEI KUNIMI,[1] KAZUHISA TSUKAMOTO,[1] NAOYUKI ISO-O,[1] JUN INATOMI,[3] HAYATO KAWAKAMI,[4] AKIHIKO KUDO,[4] HITOSHI ENDOU,[3] TAKASHI IGARASHI,[5] ATSUO GOTO,[1] TOSHIRO FUJITA,[1] AND GEORGE SEKI[1]
Departments of [1]Internal Medicine, [2]Hemodialysis and Apheresis, and [5]Pediatrics, Faculty of Medicine, Tokyo University Tokyo 113-0033; and Departments of [3]Pharmacology and Toxicology, and [4]Anatomy, Kyorin University School of Medicine, Mitaka, Tokyo 181-8611, Japan

Submitted 11 April 2002; accepted in final form 14 November 2002

Satoh, Hiroaki, Nobuo Moriyama, Chiaki Hara, Hideomi Yamada, Shoko Horita, Motoei Kunimi, Kazuhisa Tsukamoto, Naoyuki Iso-o, Jun Inatomi, Hayato Kawakami, Akihiko Kudo, Hitoshi Endou, Takashi Igarashi, Atsuo Goto, Toshiro Fujita, and George Seki. Localization of Na^+-HCO_3^- cotransporter (NBC-1) variants in rat and human pancreas. *Am J Physiol Cell Physiol* 284: C729–C737, 2003. First published November 20, 2002; 10.1152/ajpcell.00166.2002.—Mutations in Na^+-HCO_3^- cotransporter (NBC-1) cause proximal renal tubular acidosis (pRTA) associated with ocular abnormalities. One pRTA patient had increased serum amylase, suggesting possible evidence of pancreatitis. To further delineate a link between NBC-1 inactivation and pancreatic dysfunction, immunohistochemical analysis was performed on rat and human pancreas using antibodies against kidney-type (kNBC-1) and pancreatic-type (pNBC-1) transporters. In rat pancreas, the anti-pNBC-1 antibody labeled acinar cells and both apical and basolateral membranes of medium and large duct cells. In human pancreas, on the other hand, the anti-pNBC-1 antibody did not label acinar cells, although it did label the basolateral membranes of the entire duct system. The labeling by anti-kNBC-1 antibody was detected in only a limited number of rat pancreatic duct cells. To examine the effects of pRTA-related mutations, R342S and R554H, on pNBC-1 function, we performed functional analysis and found that both mutants had reduced transport activities compared with the wild-type pNBC-1. These results indicate that pNBC-1 is the predominant variant that mediates basolateral HCO_3^- uptake into duct cells in both rat and human pancreas. The loss of pNBC-1 function is predicted to have significant impact on overall ductal HCO_3^- secretion, which could potentially lead to pancreatic dysfunction.

Na^+-HCO_3^- cotransporter; pRTA; pancreatic duct cells; pancreatitis

THE NA^+-HCO_3^- COTRANSPORTER (NBC-1), originally cloned from amphibian kidney (32), has multiple functions. In the renal proximal tubules, it mediates HCO_3^- efflux from cells (7, 36, 42), whereas in other epithelial cells, such as the pancreatic duct cells and the corneal endothelium, it mediates HCO_3^- influx into cells (22, 23, 41). The expression of NBC-1 in nonepithelial cells such as trabecular meshwork cells or neurons has been also demonstrated (35, 40). Up to now, three NBC-1 variants have been identified: kNBC-1 from kidney, pNBC-1 from pancreas, and hNBC-1 from heart. Although kNBC-1 differs from pNBC-1 only at the NH_2 terminus, pNBC-1 is identical to hNBC-1 at the amino acid level and differs only in its 5′-untranslated region (1, 8, 10). These NBC-1 variants originate from the same SLC4A4 gene by alternative splicing (2). It is therefore predictable that mutational inactivation of NBC-1 variants may induce a variety of clinical manifestations, including renal and extrarenal phenotypes. Indeed, we have recently shown that mutations in the common coding region of NBC-1, corresponding to R298S and R510H in kNBC-1 or R342S and R554H in pNBC-1, cause renal proximal tubular acidosis (pRTA) associated with ocular abnormalities such as band keratopathy, glaucoma, and cataracts (19). The expression study in ECV304 cells showed that the kidney-type mutants, R298S and R510H, have reduced transport activities compared with the wild-type kNBC-1 (19). The expression of both kNBC-1 and pNBC-1 in several ocular tissues has been confirmed (6, 40). It remains to be clarified, however, whether the pancreatic-type mutants also have impaired functions, contributing to the clinical manifestations of pRTA patients.

The classic view of HCO_3^- secretion by the pancreatic duct cells had emphasized the roles of a basolateral Na^+/H^+ exchanger, intracellular HCO_3^- formation catalyzed by carbonic anhydrase, and an apical Cl^-/HCO_3^- exchanger (4). However, a functional study in guinea pig pancreatic duct cells has shown that the Na^+-HCO_3^- cotransporter contributes ~75% of HCO_3^- uptake during stimulation by secretin (22). In addition, Shumaker et al. (37) have shown that NBC-1 is respon-

Address for reprint requests and other correspondence: G. Seki, Dept. of Internal Medicine, Faculty of Medicine, Tokyo Univ., 7-3-1 Hongo, Bunkyo-ku, Tokyo 113-0033, Japan (E-mail: georgeseki-tky@umin.ac.jp).

The costs of publication of this article were defrayed in part by the payment of page charges. The article must therefore be hereby marked "*advertisement*" in accordance with 18 U.S.C. Section 1734 solely to indicate this fact.

sible for secretin-stimulated HCO_3^- uptake into human pancreatic duct cells. They have further proposed that the defect in HCO_3^- secretion during secretin stimulation in patients with cystic fibrosis (CF) is at least partly due to lack of HCO_3^- uptake via NBC-1 (37). If NBC-1 indeed plays a pivotal role in overall ductal HCO_3^- secretion, its inactivation could theoretically lead to pancreatic dysfunction as analogous to the situation in CF. Consistent with this speculation, one pRTA patient with a R298S mutation in kNBC-1 had elevated serum amylase concentrations (19, 21). Her serum amylase has remained elevated as high as three times that of the upper normal level for more than 8 yr. The clinical analysis revealed that her elevated amylase is of pancreatic origin, although this female patient, 24 yr old now, has no clinical signs of severe pancreatitis yet (Igarashi T, unpublished observation). The previous immunological studies have shown the presence of NBC-1 in rat and human pancreatic tissues (27, 38). However, the relative importance of NBC-1 variants in pancreatic HCO_3^- secretion has not been definitely determined, because the antibodies used in these studies were raised against the common NBC-1 epitopes and could not discriminate between kNBC-1 and pNBC-1 (27, 38). The aim of the present study was to further delineate a possible link between NBC-1 inactivation and pancreatic dysfunction. To this end, we first performed immunological analysis of human and rat pancreas using the variant specific anti-NBC-1 antibodies (40). Because the results clearly showed that pNBC-1 is the dominant variant in pancreatic HCO_3^- secretion, we next performed functional analysis to investigate the impacts of disease-causing mutations on the transport activity of pNBC-1.

METHODS

Immunohistochemistry. Affinity-purified anti-kNBC-1 and anti-pNBC-1 antibodies were used to determine the localization of NBC-1 variants in pancreas. They are polyclonal antibodies against the NH_2-terminal regions of human kNBC-1 (amino acids 4–16) or pNBC-1 (amino acids 2–12). The generation and specificity of these antibodies have been described elsewhere (40). Male Wistar rats were anesthetized with pentobarbital, and the pancreas was quickly removed and immersed in 4% paraformaldehyde in phosphate-buffered saline (PBS), pH 7.4. The specimens were then permeated by sequential incubation in PBS containing 10, 20, and 30% sucrose, embedded into Tissue-Tek OCT (Miles, Naperville, IL), and quickly frozen in liquid nitrogen. Sections 5 μm thick were prepared, air-dried, and immersed in PBS. Paraffin-embedded human pancreatic tissues were obtained with full informed consent from three patients who underwent the total pancreatectomy for the pancreatic carcinoma. The specimens had been immediately immersed in 10% formalin solution and then embedded in paraffin according to the standard method. Only areas that were confirmed to be histologically normal were used for the study. Sections 5 μm thick were cut from paraffin-embedded tissue blocks, rehydrated with xylene and graded alcohols, and immersed in PBS.

The immunofluorescence detection method was used for the immunohistological analysis. In brief, the rat pancreatic specimens were treated with normal goat serum (Jackson ImmunoResearch Laboratories, West Grove, PA) to block nonspecific protein binding, followed by incubation with anti-kNBC-1 or anti-pNBC-1 antibodies (1:200 dilution in PBS) overnight at 4°C. Antigen deterioration in formalin-fixed, paraffin-embedded preparations is known to result in false negative findings. Therefore, for the paraffin-embedded human specimens, antigen retrieval by autoclave (121°C, 10 min in 0.01 mol/l citrate buffer, pH 6.0), which had been shown to be extremely useful in retrieving the masked antigenicity of proteins in paraffin sections (24), was adopted. After this pretreatment, the specimens were processed similarly as described for the rat pancreas. The rat and human specimens were subsequently incubated with the mixture of Alexa Fluora 488 goat anti-rabbit IgG (H + L), Alexa Fluora 568 phalloidin for labeling of actin, and TO-PROR-3 iodide for labeling of nuclei (all from Molecular Probes, Eugene, OR) for 60 min at room temperature. After being washed with PBS, the specimens were observed with a confocal laser scanning microscope (MRC-1024K, Japan Bio-Rad Laboratories, Tokyo, Japan).

Transient expression of pNBC-1 and mutants. The wild-type human kNBC-1 and the kidney-type mutants, R298S and R510H, were cloned into a eukaryotic expression vector pcDNA3.1 (Invitrogen, San Diego, CA) (19) and designated as pkNBC, pR298S, and pR510H, respectively. The pcDNA3.1 containing the wild-type human pNBC-1 was constructed as follows (18). The DNA fragment spanning the pNBC-1 specific region was amplified by PCR from the cDNA of human corneal endothelial cells (41). This fragment was subcloned into the *Eco*RI sites of pcDNA3.1 in an appropriate orientation and designated as ppNBC-1-pre. The DNA fragment containing the remaining common region of NBC-1 was purified after digestion of pkNBC with *Afl*II and subcloned into the *Afl*II sites of ppNBC-1-pre. pcDNA3.1 containing the pancreatic-type mutants, R342S and R554H, was similarly constructed using pR298S and pR510H, respectively.

ECV304 cells were maintained in Medium199 (Life Technologies, Grand Island, NY) supplemented with 10% fetal bovine serum (Life Technologies). Cells were seeded onto 6-mm round coverslips and transfected with wild-type pNBC-1, R342S, or R554H using LipofectAMINE 2000 (Life Technologies) according to the manufacturer's instruction. In brief, cells were transfected with an equal amount of DNA in a 1:1 mixture of medium 199 and Opti-MEM I (Life Technologies) containing LipofectAMINE 2000 for 5 h. After the cells were incubated in medium199 supplemented with 10% FBS for 48 h, cell pH (pH_i) measurement and Western blot analysis were performed.

pH_i measurement. Cell-coated coverslips were incubated with HCO_3^--free, *N*-2-hydroxyethylpiperazine-*N*′-2-ethanesulfonic acid (HEPES)-buffered Ringer solution containing 10 μmol/l 2′,7′-bis(2-carboxyethyl)-5(6)-carboxyfluorescein (BCECF)-AM for 30–60 min at room temperature. The coverslip was transferred into a chamber mounted on an inverted microscope (IMT-2, Olympus, Tokyo, Japan). We noticed that ECV304 cells have a significant activity of Na^+-dependent Cl^-/HCO_3^- exchanger, which could interfere with the assessment of NBC-1 activities. Therefore, the coverslip was superfused for 30 min at ~5 ml/min with Cl^--free HCO_3^- solution containing (in mmol/l) 144 Na^+, 5 K^+, 5 Ca^{2+}, 1 Mg^{2+}, 132 gluconate$^-$, 2 $H_2PO_4^-$, 1 SO_4^{2-}, 25 HCO_3^-, and 5.5 glucose to reduce intracellular Cl^-. Our preliminary experiments confirmed that this treatment was sufficient to minimize the influence of Na^+-dependent Cl^-/HCO_3^- exchange activity. pH_i was measured with a microscopic fluorescence photometry system (OSP-10, Olympus) as previously described (18, 41). The intracellular dye was alternately excited

at two wavelengths (440 and 490 nm), and emission was measured at a wavelength of 530 nm. Autofluorescence of cells was measured at the beginning of an experimental day, and these values were subtracted from the raw data. We used 10 μmol/l nigericin to acidify the cells. This method has been shown to induce a more stable and predictable acidification than the NH_4Cl-pulse technique, especially in Cl^--free solution (18, 40). We have confirmed that Na^+/H^+ exchange activity assayed by the nigericin acidification was identical to that assayed by the NH_4Cl-pulse technique (18, 40). Therefore, the problem of proton leak that might be caused by residual nigericin has been shown to be minimal, if any, in our system. After cell acidification, the coverslip was superfused for 3–4 min with Na^+-free, Cl^--free HCO_3^- solution (Na^+ was replaced with *N*-methyl-D-glucamine). Thereafter, pH_i recovery was induced by Cl^--free HCO_3^- solution containing 1 mmol/l amiloride that completely inhibits an endogenous Na^+/H^+ exchange activity as described (19). In some experiments, Cl^--free HCO_3^- solution containing both 1 mmol/l amiloride and 0.3 mmol/l 4,4′-diisothiocyanostilbene-2,2′-disulfonic acid (DIDS) was used to confirm that the Na^+-induced pH_i recovery in this condition is due to NBC-1 activity (8, 19). The calibration curve for pH_i was made according to the method by Thomas et al. (39). In brief, cells were exposed to HEPES-buffered solution containing 120 mmol/l K^+ and 10 μmol/l nigericin. Solution pH was adjusted at the different levels (from 6.4 to 7.8) with 1 N NaOH, whereas Na^+ concentration in solution was kept constant at 20 mmol/l as previously reported (28). Throughout the paper, the results are expressed as mean values ± SE. ANOVA with Bonferroni's adjustment was used for multiple comparisons of data, and a P value of <0.05 was considered statistically significant. BCECF-AM was obtained from Dojindo (Kyushu, Japan), and DIDS, amiloride, and nigericin were from Sigma Chemical (St. Louis, MO). All other chemicals were from Wako Pure Chemicals Industries (Osaka, Japan) unless otherwise specified.

Western blot analysis. Pancreas and kidneys were removed from Wistar rats and immediately homogenized in ice-cold buffer containing 280 mmol/l sucrose and 0.2 mmol/l Pefabloc SC (Boehringer Mannheim, Mannheim, Germany). The plasma membrane fraction was obtained by differential and discontinuous sucrose gradient procedures as described (18). Protein samples were boiled for 5 min in sample buffer, separated by SDS-PAGE on 7% acrylamide minigels, and blotted onto a nitrocellulose membrane. After incubation in blocking buffer, the membrane was treated with the diluted anti-NBC-1 antibodies (1:200) and then with horseradish peroxidase-conjugated anti-rabbit IgG (Bio-Rad, Richmond, CA) as the secondary antibody. The signal was detected by an ECL Plus system (Amersham, Aylesbury, UK).

Two days after transfection, ECV304 cells were lysed and the plasma membrane fraction was obtained. An equal amount of protein samples (50 μg/lane) was processed for Western blot analysis, as described above, using the antibody against NBC-1 COOH-terminal region (18) as the primary antibody.

Reverse transcription-polymerase chain reaction. For reverse transcription-polymerase chain reaction (RT-PCR) analysis, total RNA was isolated from freshly isolated rat kidney and pancreas using the guanidinium isothiocyanate and phenol-chloroform extraction method described by Chomczynski and Sacchi (12). Primers were designed from the rat kNBC-1 sequence (9) as follows: 5′-GAT GTC CAC TGA AAA TGT GGA-3′ (sense primer) and 5′-AGC ATG ACA GCC CTG CTC TGA-3′ (antisense primer). These primers were set to amplify the kNBC-1 specific region and a part of the NBC-1 common region. The conditions for PCR were as follows: 30 cycles of 30 s at 94°C, 30 s at 60°C, and 45 s at 72°C, with an initial 9-min denaturing step and a final 5-min elongation step.

RESULTS

Western blot analysis. To determine the dominant NBC-1 variant in pancreas, we first performed Western blot analysis. For human pancreas, we could obtain only paraffin-embedded specimens, which were not suitable for Western blot analysis. Therefore, Western blot was performed only on rat pancreas. As shown in Fig. 1, the anti-pNBC-1 antibody recognized a ~145-kDa band on immunoblots of rat pancreas. On the other hand, the anti-kNBC-1 antibody did not recognize a significant band in rat pancreas, although this antibody did recognize a prominent band at ~130 kDa in rat kidney. These results suggest that pNBC-1 is the dominant variant in pancreas. A recent study also reported that the apparent molecular weight of pNBC-1 expressed in pancreas is slightly larger than that of kNBC-1 expressed in kidney (6). The molecular weight of pNBC-1 predicted from its cDNA is ~121 kDa (1), whereas that of kNBC-1 is ~116 kDa (8), suggesting that NBC-1 proteins are posttranslationally modified in slightly different ways in pancreas and kidney. Consistent with this view, the antibody against the NBC-1 COOH-terminal region that recognizes both kNBC-1 and pNBC-1 (18) yielded a ~130-kDa band in rat kidney but a ~145-kDa band in rat pancreas (data not shown).

Localization of NBC-1 variants in rat and human pancreas. We next examined localization of NBC-1 variants in pancreas with the immunofluorescence detection method using confocal microscopy. Consistent with the results of Western blot analysis, the expression of pNBC-1 appeared dominant in both rat and human pancreas. However, there was a significant species difference in the patterns of pNBC-1 expression. The anti-pNBC-1 and anti-kNBC-1 antibodies did not label the islet cells in both rat and human pancreas.

In rat pancreas, the anti-pNBC-1 antibody labeled the acinar cells and the duct cells (Fig. 2, *a* and *b*). The nonimmunized rabbit IgG gave no fluorescence signals.

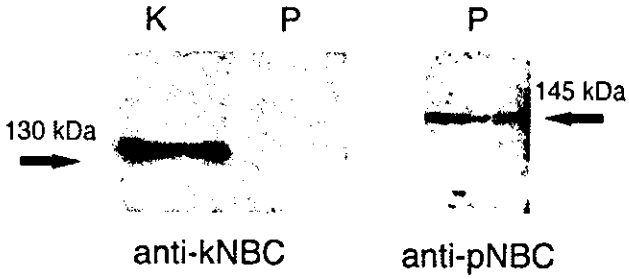

Fig. 1. Western blot analysis on rat kidney and pancreas. *Left*: the results by the anti-kidney Na^+-HCO_3^- cotransporter (kNBC-1) antibody. *Right*: the results by the anti-pancreatic NBC-1 (pNBC-1) antibody. K, kidney (100 μg/lane); P, pancreas (100 μg/lane).

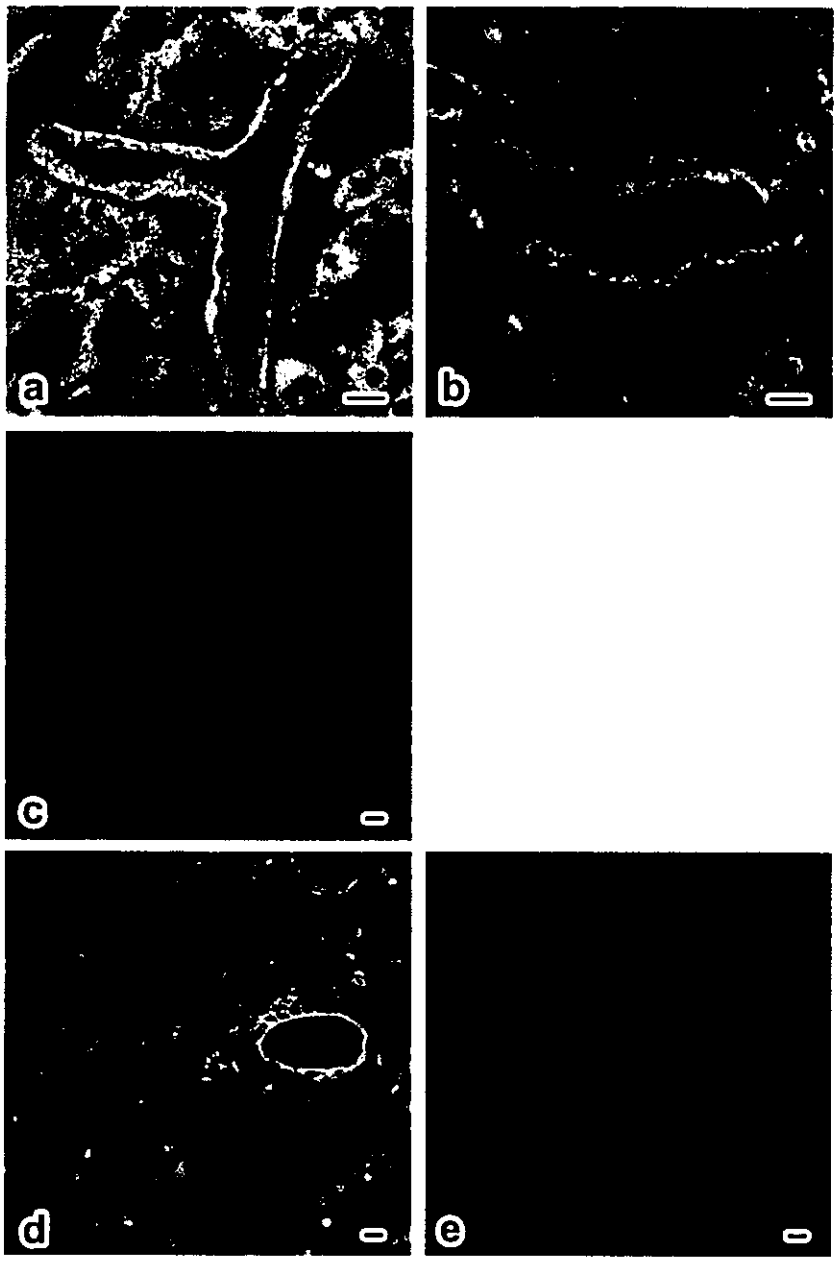

Fig. 2. Immunolocalization of NBC-1 isoforms in rat pancreas. Green shows the localization of NBC-1, red shows actin, and blue shows nuclei. *a–c*: labeling by anti-pNBC-1 antibody. Although the labeling in acini is basolaterally dominant (*a*), the labeling in duct cells is observed in both basolateral (*a*) and apical (*b*) sides. The labeling is diminished in the presence of the corresponding antigen (*c*). *d* and *e*: labeling by anti-kNBC-1 antibody. Occasional labeling is observed in the apical side of duct cells (*d*) and is diminished in the presence of the corresponding antigen (*e*). Bar indicates 10 μm.

Furthermore, the labeling by the anti-pNBC-1 antibody was diminished in the presence of antigen peptide (Fig. 2*c*), confirming the specificity of immunoreactions. In the acinar cells, the labeling appeared basolaterally dominant (Fig. 2*a*). In the medium and large ducts, such as the interlobular and the main ducts, the labeling was observed on both apical and basolateral membranes (Fig. 2, *a* and *b*), although the apical staining was less intense than the basolateral staining. In the intralobular ducts, the labeling was not so prominent and most of the intercalated ducts were not labeled. The anti-kNBC-1 antibody did not label the acinar cells, although it did label a limited number of the medium and large ducts (Fig. 2*d*). This occasional ductal labeling by anti-kNBC-1 antibody appeared rather apically dominant and was diminished in the presence of antigen peptide.

In human pancreas, in contrast, the anti-pNBC-1 antibody did not label the acinar cells. Instead, this antibody quite intensively labeled the small intercalated cells (Fig. 3*a*). Higher magnification (Fig. 3*c*) and Nomarski-differential interference microscopic image (Fig. 3*d*) show that this labeling was dominant in the basolateral membranes of small ducts but was not observed in acinar cells. The labeling was diminished in the presence of antigen peptide (Fig. 3*d*). The anti-

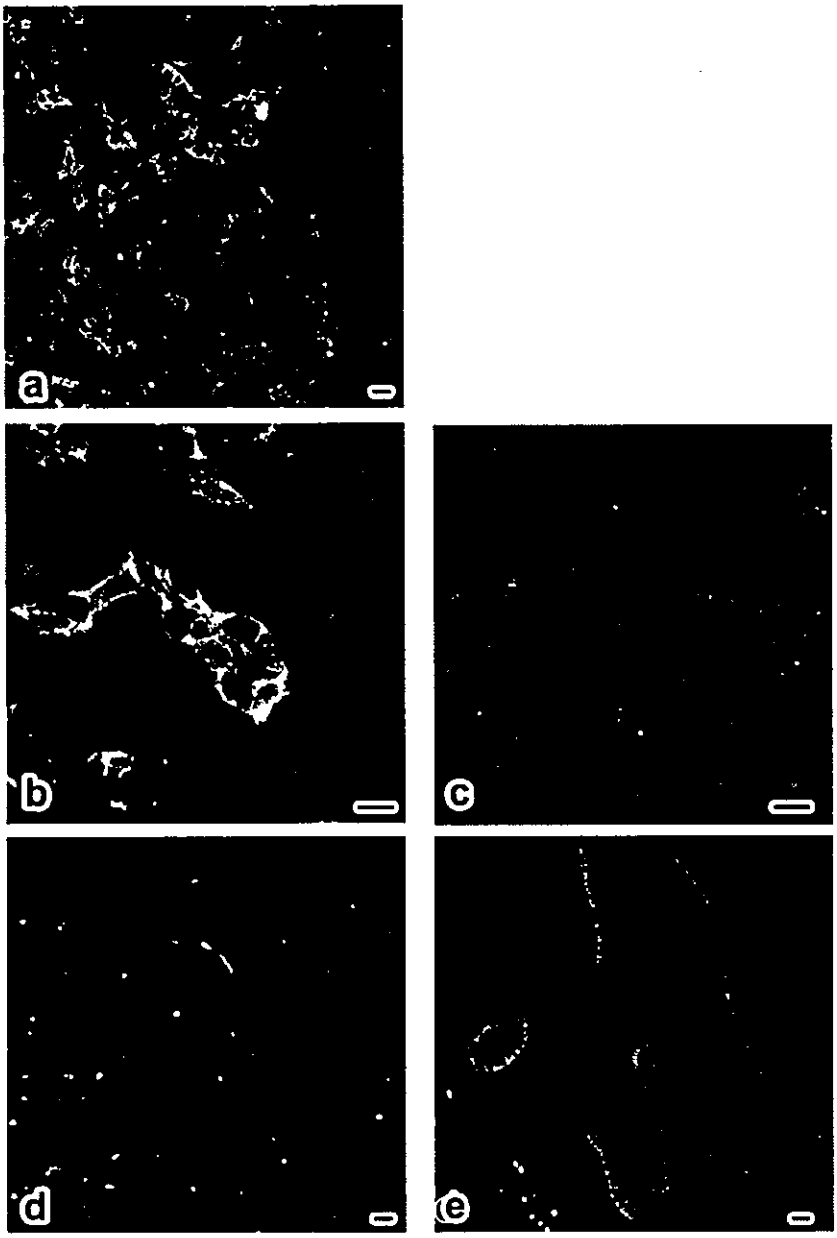

Fig. 3. Immunolocalization of pNBC-1 in human pancreas. The labeling by anti-pNBC-1 antibody is observed in the intercalated duct cells but not in the acinar cells (*a*). Higher magnification shows that this labeling is basolaterally dominant (*b*). Nomarski-differential interference microscopic image confirms that the labeling is confined to the small ducts and is not observed in acinar cells (*c*). The labeling is diminished in the presence of the corresponding antigen (*d*). In larger duct cells, the pNBC-1 labeling is also basolaterally dominant (*e*). Details as in Fig. 2.

pNBC-1 antibody also labeled the medium and large ducts, such as the intralobular, the interlobular, and the main ducts, and the labeling of these ducts appeared to be confined to the basolateral membranes (Fig. 3*e*). The labeling by anti-kNBC-1 antibody was not observed in human pancreas.

Detection of kNBC-1 mRNA in rat pancreas. The anti-kNBC-1 antibody did not yield a clear band in Western blot analysis, although it did label a limited number of ducts in rat pancreas. This suggests that a small amount of kNBC-1 mRNA is expressed in rat pancreas. To test for this view, we performed RT-PCR analysis. As shown in Fig. 4, RT-PCR on the kNBC-1

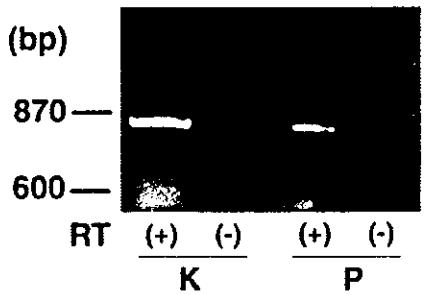

Fig. 4. The expression of kNBC-1 mRNA in rat kidney and pancreas. RT-PCR analysis with (+) or without (−) the reverse transcription (RT) step. K, rat kidney; P, rat pancreas.

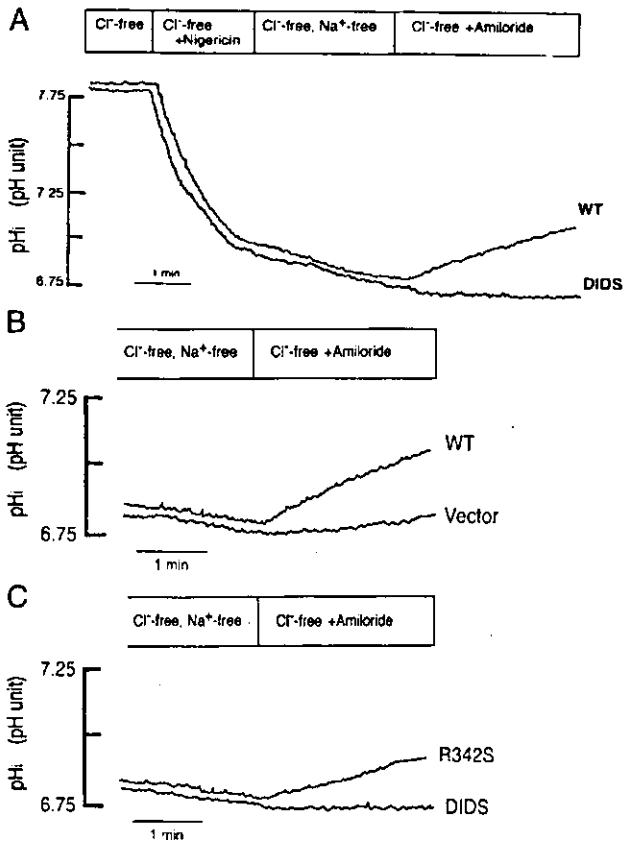

Fig. 5. Cell pH (pH_i) recovery from acid load in ECV304 cells. Cells transfected with the wild-type pNBC-1 (WT) were acidified by nigericin in Cl^--free HCO_3^- solution, and then Na^+ was removed from the perfusate. pH_i recovery was induced by readdition of Na^+ in the presence of 1 mmol/l amiloride with or without 0.3 mmol/l DIDS (*A*). Results from cells transfected with vector alone (Vector) or with the wild-type pNBC-1 are shown (*B*). Results from cells transfected with R342H in the absence and presence of 0.3 mmol/l DIDS are shown (*C*).

specific region yielded a band of the expected size (800 bp) from rat pancreas as well as from rat kidney.

Functional analysis of pNBC-1 mutants. These immunohistological findings indicate that pNBC-1 is the dominant variant in both rat and human pancreas. Because one patient with a NBC-1 missense mutation presented high serum amylase levels, we decided to examine whether disease-causing mutations (19) affect the transport activity of pNBC-1. To accomplish this task, we transiently expressed the wild-type pNBC-1 or the R342S or R554H mutants in ECV304 cells and compared the rates of DIDS-sensitive pH_i recovery from acid-load in Cl^--free HCO_3^- solution. After acidification by nigericin, the cells did not show any pH_i recovery in the absence of ambient Na^+. When Na^+ was reintroduced together with amiloride, however, the cells transfected with the wild-type pNBC-1 showed a prompt pH_i recovery as shown in Fig. 5*A*, which was completely inhibited by 0.3 mmol/l DIDS (n = 6). On the other hand, the cells transfected with vector alone showed little pH_i recovery (Fig. 5*B*). To

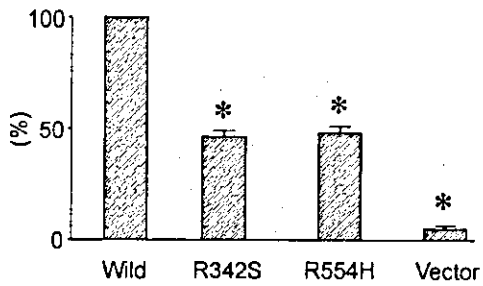

Fig. 6. Transport activities of the wild-type pNBC-1 and the mutants. DIDS-sensitive pH_i recovery rate from acidification (dpH_i/dt) was 0.073 ± 0.004, 0.035 ± 0.003, 0.034 ± 0.004, and 0.006 ± 0.001 pH unit/min in cells transfected with the wild-type (Wild, n = 22), R342S (n = 10), R554H (n = 11), and vector (n = 10), respectively. The dpH_i/dt value in each cell was expressed as a percentage of that in the wild type. The recovery from acidification was significantly reduced in R342S and R554H mutants. *$P < 0.005$ from wild type.

confirm that the Na^+-induced pH_i recovery in Cl^--free HCO_3^- solution indeed reflects the pNBC-1 activity, the similar experiments were performed in the absence of CO_2/HCO_3^- using HEPES-buffered Cl^--free solution. In this case, readdition of Na^+ induced little pH_i recovery in both cells transfected with the wild-type pNBC-1 and vector alone. Thus the rates of pH_i recovery were 0.002 ± 0.002 pH/min for pNBC-1 (n = 8) and 0.001 ± 0.002 pH/min for vector (n = 8), and both values were not significantly different from zero. In Cl^--free HCO_3^- solution, readdition of Na^+ induced a modest pH_i recovery in cells transfected with R342S (Fig. 5*C*) or R554H, which was again completely inhibited by DIDS (n = 6 for each). Figure 6 shows the DIDS-sensitive transport activities thus analyzed at the identical pH_i level: 6.86 ± 0.02 for wild-type (n = 22), 6.85 ± 0.03 for R342S (n = 10), and 6.88 ± 0.02 for R554H (n = 11). As shown, the activities of R342S or R554H mutants were significantly reduced ($P < 0.005$) and were 49.8 ± 3.0% and 48.1 ± 3.3% of the activity of wild-type pNBC-1, respectively. As shown in Fig. 7, the protein expression of pNBC-1 was comparable among the wild-type and mutants. Densitometry analysis of three independent experiments did not reveal significant differences in the level of protein expression.

DISCUSSION

To clarify the relative importance of NBC-1 variants in pancreatic HCO_3^- secretion, we performed immunohistological analysis using anti-kNBC-1 and anti-

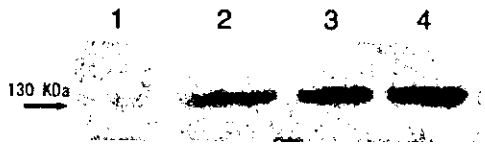

Fig. 7. Expression of the wild-type pNBC-1 and the mutants in ECV304 cells. The antibody against NBC-1 COOH terminus was used, and a representative of 3 independent blots is shown. *Lane 1*: nontransfected control cells. *Lane 2*: cells transfected with the wild-type pNBC-1. *Lane 3*: cells transfected with R342S. *Lane 4*: cells transfected with R554H.

pNBC-1 antibodies (40). The results clearly demonstrate that pNBC-1 is the dominant variant in HCO_3^- secretion in both rat and human pancreas. The anti-kNBC-1 antibody labeled the apical membranes of some ducts cells in rat pancreas, but this labeling was limited to only a small portion of duct cells. Moreover, the anti-kNBC-1 antibody, unlike the anti-pNBC-1 antibody, did not recognize a clear band by Western blot analysis on rat pancreas. We could not obtain the fresh human pancreatic tissues suitable for Western blot analysis, but the labeling by anti-kNBC-1 antibody was not detected in paraffin-embedded human pancreatic tissues. These results might reflect a species-dependent difference in the kNBC-1 expression in pancreas. Consistent with this view, a previous Northern blot analysis detected pNBC-1 mRNA but not kNBC-1 mRNA in human pancreas (1). Nevertheless, our RT-PCR analysis indicated that a small amount of kNBC-1 mRNA is really expressed in rat pancreas.

It should be pointed out that another NBC-1-related isoform (rb2NBC) has been cloned from rat brain (5). This isoform has a unique COOH terminus, but its NH_2 terminus is identical to that of pNBC-1. It could be possible, therefore, that the anti-pNBC-1 antibody used in the present study also recognizes this isoform. However, our preliminary Western blot analysis on rat pancreas using the antibody against the unique COOH-terminal region of rb2NBC failed to yield a clear band, suggesting that pNBC-1 is really the dominant variant in pancreas.

In rat pancreas, the anti-pNBC-1 antibody labeled both acinar cells and duct cells. The labeling in acinar cells was quite intense and appeared rather basolateral dominant. Whereas the antibody labeled both apical and basolateral membranes in the medium and large ducts, most of the small, intercalated ducts were not labeled. In human pancreas, on the other hand, the anti-pNBC-1 antibody did not label the acinar cells, although it did intensively label the basolateral membranes of entire duct system, including the smallest intercalated cells. In view of the high proteolytic activity of acinar cells, we cannot exclude the possibility that a small amount of pNBC-1 is also expressed in human acinar cells but is not detected by the methods employed in the present study. However, the previous immunohistological studies using the antibodies against the common NBC-1 epitopes have also reported a very similar species difference in NBC-1 expression in pancreas. Thus, in rat pancreas, Thévenod et al. (38) have reported that NBC-1 is expressed in the basolateral membranes of acinar cells and in both apical and basolateral membranes of duct cells. In human pancreas, by contrast, Marino et al. (27) have reported that NBC-1 is expressed in the basolateral membranes of duct cells but not in the acinar cells. These results and observations may suggest different fluid and electrolyte secretion mechanisms in rat and human pancreas.

A previous functional study has shown the presence of Na^+-HCO_3^- cotransport activity in rat acinar cells, which has been interpreted to be important for intracellular pH regulation (29). The cotransport activity has also been detected in the basolateral membranes of rat pancreatic ducts (43), but this finding has not been confirmed by others (31). Although Na^+-HCO_3^- cotransport activity has not been investigated in human acinar cells, the transport activity of NBC-1 has been confirmed in the human ductal pancreatic adenocarcinoma cell lines (37). Although the physiological significance of apical NBC-1 expression in rat pancreatic duct cells is not obvious at present, a similar apical NBC-1 expression has also been reported in rat submandibular and parotid glands (33). In any case, the pure basolateral localization of pNBC-1 along the entire duct system of human pancreas might be more advantageous for net HCO_3^- secretion, considering the primary role of NBC-1 as HCO_3^- uptake into duct cells (22, 37). In this regard, it would be interesting to note that the HCO_3^- concentration in secretin-stimulated pancreatic juice is much higher in human than in rat (4).

We have previously shown that missense mutations identified in pRTA patients reduce the transport activity of kNBC-1. The present study confirmed that these mutations also impair pNBC-1 function, which could potentially explain the pancreatic phenotype associated with pRTA (19, 21). We cannot exclude the possibility, however, that these mutations might also affect the targeting and/or recycling of the NBC-1 protein in human tissues. Recently, Shumaker et al. (37) have shown that both CF transmembrane conductance regulator (CFTR) and NBC-1 cooperatively function to accomplish HCO_3^- uptake into the human ductal pancreatic adenocarcinoma cell lines. According to their model, activation of CFTR by cAMP depolarizes the membrane potentials, which in turn stimulates the basolateral HCO_3^- uptake through the electrogenic Na^+-HCO_3^- cotransporter, NBC-1. The HCO_3^- is then secreted at the apical membranes via an apical Cl^-/HCO_3^- exchanger and possibly a bicarbonate conductive pathway. Pancreatic dysfunction associated with CF is thought to result primarily from impairment of secretin-stimulated ductal Cl^- and HCO_3^- secretion (17, 25). In particular, the reduction in intraductal pH will not only facilitate precipitation of proteins secreted from acinar cells but also disrupt vesicular trafficking in the apical domain of acinar cells, leading ultimately to pancreatic fibrosis and insufficiency (15, 34). Usually, typical CF patients with pancreatic insufficiency tend to have severe CFTR mutations in both alleles, among which delta F508 is most frequent, but other mutations such as G542X are also found (26). However, a subset of patients with idiopathic chronic pancreatitis has only mild CFTR mutations without other clinical features of CF (13, 14, 30). A recent elegant study by Choi et al. (11) suggests that the defect in CFTR-dependent HCO_3^- transport, but not the inactivation of CFTR Cl^- channel activity itself, may actually be responsible for the pancreatic phenotype in these cases. A study in CFTR knockout mice (16) also supports the view that acidic pH changes in luminal secretions play quite an important role in the pathogenesis of pancre-

atic dysfunction observed in CF. Because only a few NBC-1 mutations have been identified so far (3, 19, 20), a definite conclusion cannot be drawn at present as to a possible link between NBC-1 inactivation and pancreatic dysfunction. In addition, clear evidence of pancreatitis is not yet reported in another pRTA patient with S427L mutation in kNBC-1 (3). Nevertheless, it is tempting to speculate that the inactivation of pNBC-1 may, at least in some patients, decreases ductal HCO_3^- secretion similarly as in CF, leading to pancreatic dysfunction. It would be expected, in particular, that mutations in the unique NH_2-terminal region of pNBC-1 would induce a pancreatic phenotype without severe pRTA, because kNBC-1 seems to be responsible for a majority of HCO_3^- reabsorption from renal proximal tubules (1, 8). It is currently unknown whether some environmental factors modify the clinical course of pancreatic dysfunction in patients with NBC-1 mutations.

Nonalcoholic chronic pancreatitis is a potentially life-threatening disease (14). Although idiopathic pancreatitis is frequently associated with CFTR mutations, recent studies suggest that other genetic factors may be also involved (13, 30). To better understand the pathogenesis of idiopathic pancreatitis and to establish the more effective therapeutic strategy, future studies are required, including the genetic testing of pNBC-1 mutations.

We thank Kumamoto Immunochemical Laboratory (Kumamoto, Japan) for providing anti-NBC-1 antibodies.

This study was in part supported by grants 12671024 and 14571013 from the Ministry of Education, Science, and Culture of Japan.

REFERENCES

1. **Abuladze N, Lee I, Newman D, Hwang J, Boorer K, Pushkin A, and Kurtz I.** Molecular cloning, chromosomal localization, tissue distribution, and functional expression of the human pancreatic sodium bicarbonate cotransporter. *J Biol Chem* 273: 17689–17695, 1998.
2. **Abuladze N, Song M, Pushkin A, Newman D, Lee I, Nicholas S, and Kurtz I.** Structural organization of the human NBC1 gene: kNBC1 is transcribed from an alternative promoter in intron 3. *Gene* 251: 109–122, 2000.
3. **Alper SL.** Genetic diseases of acid-base transporters. *Annu Rev Physiol* 64: 899–923, 2002.
4. **Argent BE and Case RM.** Pancreatic ducts: cellular mechanism and control of bicarbonate secretion. In: *Physiology of the Gasrointestinal Tract*, edited by Johnson LR. New York: Raven, 1994, p. 1473–1497.
5. **Bevensee MO, Schmitt BM, Choi I, Romero MF, and Boron WF.** An electrogenic Na^+-HCO_3^- cotransporter (NBC) with a novel COOH terminus, cloned from rat brain. *Am J Physiol Cell Physiol* 278: C1200–C1211, 2000.
6. **Bok D, Schibler MJ, Pushkin A, Sassani P, Abuladze N, Naser Z, and Kurtz I.** Immunolocalization of electrogenic sodium-bicarbonate cotransporters pNBC1 and kNBC1 in the rat eye. *Am J Physiol Renal Physiol* 281: F920–F935, 2001.
7. **Boron WF and Boulpaep EL.** Intracellular pH regulation in the renal proximal tubule of the salamander. Basolateral HCO_3^- transport. *J Gen Physiol* 81: 53–94, 1983.
8. **Burnham CE, Amlal H, Wang Z, Shull GE, and Soleimani M.** Cloning and functional expression of a human kidney Na^+:HCO_3^- cotransporter. *J Biol Chem* 272: 19111–19114, 1997.
9. **Burnham CE, Flagella M, Wang Z, Amlal H, Shull GE, and Soleimani M.** Cloning, renal distribution, and regulation of the rat Na^+-HCO_3^- cotransporter. *Am J Physiol Renal Physiol* 274: F1119–F1126, 1998.
10. **Choi I, Romero MF, Khandoudi N, Bril A, and Boron WF.** Cloning and characterization of a human electrogenic Na^+-HCO_3^- cotransporter isoform (hhNBC). *Am J Physiol Cell Physiol* 276: C576–C584, 1999.
11. **Choi JY, Muallem D, Kiselyov K, Lee MG, Thomas PJ, and Muallem S.** Aberrant CFTR-dependent HCO_3^- transport in mutations associated with cystic fibrosis. *Nature* 410: 94–97, 2001.
12. **Chomczynski P and Sacchi N.** Single-step method of RNA isolation by acid guanidinium thiocyanate-phenol-chloroform extraction. *Anal Biochem* 162: 156–159, 1987.
13. **Cohn JA, Friedman KJ, Noone PG, Knowles MR, Silverman LM, and Jowell PS.** Relation between mutations of the cystic fibrosis gene and idiopathic pancreatitis. *N Engl J Med* 339: 653–658, 1998.
14. **Etemad B and Whitcomb DC.** Chronic pancreatitis: diagnosis, classification, and new genetic developments. *Gastroenterology* 120: 682–707, 2001.
15. **Freedman SD, Kern HF, and Scheele GA.** Acinar lumen pH regulates endocytosis, but not exocytosis, at the apical plasma membrane of pancreatic acinar cells. *Eur J Cell Biol* 75: 153–162, 1998.
16. **Freedman SD, Kern HF, and Scheele GA.** Pancreatic acinar cell dysfunction in CFTR(−/−) mice is associated with impairments in luminal pH and endocytosis. *Gastroenterology* 121: 950–957, 2001.
17. **Gaskin KJ, Durie PR, Corey M, Wei P, and Forstner GG.** Evidence for a primary defect of pancreatic HCO_3^- secretion in cystic fibrosis. *Pediatr Res* 16: 554–557, 1982.
18. **Hara C, Satoh H, Usui T, Kunimi M, Noiri E, Tsukamoto K, Taniguchi S, Uwatoko S, Goto A, Racusen LC, Inatomi J, Endou H, Fujita T, and Seki G.** Intracellular pH regulatory mechanism in a human renal proximal cell line (HKC-8): evidence for Na^+/H^+ exchanger, Cl^-/HCO_3^- exchanger and Na^+-HCO_3^- cotransporter. *Pflügers Arch* 440: 713–720, 2000.
19. **Igarashi T, Inatomi J, Sekine T, Cha SH, Kanai Y, Kunimi M, Tsukamoto K, Satoh H, Shimadzu M, Tozawa F, Mori T, Shiobara M, Seki G, and Endou H.** Mutations in SLC4A4 cause permanent isolated proximal renal tubular acidosis with ocular abnormalities. *Nat Genet* 23: 264–266, 1999.
20. **Igarashi T, Inatomi J, Sekine T, Seki G, Shimadzu M, Tozawa F, Takeshima Y, Takumi T, Takahashi T, Yoshikawa N, Nakamura H, and Endou H.** Novel nonsense mutation in the Na^+/HCO_3^- cotransporter gene (SLC4A4) in a patient with permanent isolated proximal renal tubular acidosis and bilateral glaucoma. *J Am Soc Nephrol* 12: 713–718, 2001.
21. **Igarashi T, Ishii T, Watanabe K, Hayakawa H, Horio K, Sone Y, and Ohga K.** Persistent isolated proximal renal tubular acidosis–a systemic disease with a distinct clinical entity. *Pediatr Nephrol* 8: 70–71, 1994.
22. **Ishiguro H, Steward MC, Lindsay AR, and Case RM.** Accumulation of intracellular HCO_3^- by Na^+-HCO_3^- cotransport in interlobular ducts from guinea-pig pancreas. *J Physiol* 495: 169–178, 1996.
23. **Jentsch TJ, Keller SK, Koch M, and Wiederholt M.** Evidence for coupled transport of bicarbonate and sodium in cultured bovine corneal endothelial cells. *J Membr Biol* 81: 189–204, 1984.
24. **Kawai K, Serizawa A, Hamana T, and Tsutsumi Y.** Heat-induced antigen retrieval of proliferating cell nuclear antigen and p53 protein in formalin-fixed, paraffin-embedded sections. *Pathol Int* 44: 759–764, 1994.
25. **Kopelman H, Corey M, Gaskin K, Durie P, Weizman Z, and Forstner G.** Impaired chloride secretion, as well as bicarbonate secretion, underlies the fluid secretory defect in the cystic fibrosis pancreas. *Gastroenterology* 95: 349–355, 1988.
26. **Kristidis P, Bozon D, Corey M, Markiewicz D, Rommens J, Tsui LC, and Durie P.** Genetic determination of exocrine pancreatic function in cystic fibrosis. *Am J Hum Genet* 50: 1178–1184, 1992.
27. **Marino CR, Jeanes V, Boron WF, and Schmitt BM.** Expression and distribution of the Na^+-HCO_3^- cotransporter in human